DOT/FAA/AR-99/24

Office of Aviation Research
Washington, D.C. 20591

Structural Integrity of Discontinuous Stiffened Integrally Braided and Woven Composite Panels

March 1999

Final Report

U.S. Department of Transportation
Federal Aviation Administration

NOTICE

This document is disseminated under the sponsorship of the U.S. Department of Transportation in the interest of information exchange. The United States Government assumes no liability for the contents or use thereof. The United States Government does not endorse products or manufacturers. Trade or manufacturer's names appear herein solely because they are considered essential to the objective of this report. This document does not constitute FAA certification policy. Consult your local FAA aircraft certification office as to its use.

This report is available at the Federal Aviation Administration William J. Hughes Technical Center's Full-Text Technical Reports page: www.tc.faa.gov/its/act141/reportpage.html in Adobe Acrobat portable document format (PDF).

Technical Report Documentation Page

1. Report No.	2. Government Accession No.	3. Recipient's Catalog No.
DOT/FAA/AR-99/24		

4. Title and Subtitle	5. Report Date
STRUCTURAL INTEGRITY OF DISCONTINOUS STIFFENED INTEGRALLY BRAIDED AND WOVEN COMPOSITE PANELS	March 1999
	6. Performing Organization Code

7. Author(s)	8. Performing Organization Report No.
K. N. Shivakumar, M. J. Sundaresan, and V. S. Avva	

9. Performing Organization Name and Address	10. Work Unit No. (TRAIS)
Center for Composite Materials Research Department of Mechanical Engineering North Carolina A&T State University 1601 East Market Street Greensboro, NC 27411	11. Contract or Grant No. Grant No. FAA 95-G-013

12. Sponsoring Agency Name and Address	13. Type of Report and Period Covered
U.S. Department of Transportation Federal Aviation Administration Office of Aviation Research Washington, DC 20591	Final Report
	14. Sponsoring Agency Code AIR-120

15. Supplementary Notes

Federal Aviation Administration William J. Hughes Technical Center Technical Monitor is Peter Shyprykevich.

16. Abstract

The strength and failure modes of discontinuous blade stiffened panels made of textile preform composites (three-dimensional (3D) braided (0°/±17°) and 3D orthogonal woven (0°/90°/90°)) were evaluated through 3D finite element analysis and test. Tests were conducted under quasi-static tensile and tension-tension fatigue conditions. The peel and shear stresses at the notch root were as high as 40% and 80% of the axial stress, and they caused failure initiation. Final static fracture in both braided and woven composite panels were by net section tensile failure. The average strengths of the braided and the woven panels were 433.7 MPa and 581.8 MPa, respectively. However, the initial failure of the woven panels was stiffener separation but because the load carried by the blade stiffener was only about 10% of the total load, the panels were able to carry additional load until final failure occurred in tension. The stiffener separation occurred at about 28% of the final failure load (162.7 MPa). This load level is considered as the useful capability of the panel. Thus the behavior of the woven panels was similar to the conventional tape construction. The two specimens that were tested under fatigue (S_{max} = 0.6 S_{ult} and R = 0.1) survived one million cycles, but the woven panel lost its stiffener, and the residual strength of braided and woven composite specimens were 88.6% and 90.9% of their respective static strengths.

17. Key Words	18. Distribution Statement
Textile composites, Three-dimensional braided composites, Three-dimensional orthogonal woven composites, Stiffened panel, Stiffener discontinuity, Fracture strength, Fatigue limit, Finite element analysis	This document is available to the public through the National Technical Information Service (NTIS), Springfield, Virginia 22161.

19. Security Classif. (of this report)	20. Security Classif. (of this page)	21. No. of Pages	22. Price
Unclassified	Unclassified	58	

Form DOT F1700.7 (8-72) Reproduction of completed page authorized

TABLE OF CONTENTS

LIST OF ILLUSTRATIONS

LIST OF TABLES

EXECUTIVE SUMMARY

Textile preform composites offer cost, processing, and performance advantages compared to conventional laminated composites. Hence, textile composites are attractive candidates for construction of the stiffened panels widely used in airframe structures. In such applications, the stiffener discontinuity induces high levels of interlaminar stresses. When the stiffened panels are fabricated from conventional laminated composite materials, stresses at the stiffener terminations lead to premature failure of the panels. The superior strength and damage tolerance of the integrally braided and woven textile preform composites are likely to be assets in such situations.

The objective of this study was to evaluate the structural integrity of discontinuous blade-stiffened panels made of textile preform composites and to compare their strength and failure modes with those of conventional laminated stiffened panels. Three-dimensional (3D) braided ($0°/\pm17°$) and 3D orthogonal woven ($0°/90°/90°$) composite panels made of BASF G30-500 graphite fiber yarns and Dow Chemical's Tactix-123 matrix were evaluated. Resin transfer molding was used for fabricating the stiffened panels. Specimens were fabricated and tested under quasi-static tension and tension-tension fatigue.

Five braided composite panels and five woven composite panels were tested under quasi-static tension to identify failure initiation, failure modes, and final fracture. These specimens were instrumented with strain gages and the strains were continuously monitored during the tests. The maximum peel and shear stresses at the notch root were about 40% and 80% of the axial stress and they caused failure initiation. In braided composite specimens, failure was initiated by peel stresses and in woven specimens by shear stresses leading to stiffener separation or disbond. Final fracture of both braided and woven composite panels were by net section tensile failure. The average strengths at final failure of the braided and the woven panels were 433.7 MPa and 581.8 MPa, respectively. However, the initial failure of the woven panels was stiffener separation but because the load carried by the blade stiffener was only about 10% of the total load, the panels were able to carry additional load in the skin of the panel until final failure occurred in tension. The stiffener separation occurred at about 28% of the final failure load (162.7 MPa). This load level is considered as the useful capability of the panel. Thus the behavior of the woven panels were similar to the conventional tape construction while the braided panel avoided the stiffener separation failure mode.

One braided and one woven composite specimen were tested under tension-tension fatigue with a stress value of $S_{max} = 0.6\ S_{ult}$ and a stress ratio of 0.1. The damage accumulation was measured through the compliance change of the specimen. Both the braided and the woven specimens survived one million fatigue cycles, but the woven panel lost its stiffener. The change in compliances for the braided and woven composite specimens in one million cycles was 9.27% and 7.83%, respectively. The residual strengths of braided and woven composite specimens were 384.2 MPa and 528.7 MPa, respectively, which are 88.6% and 90.9% of their corresponding average static strengths.

To identify the regions of high stresses and to design the test specimen with stiffener discontinuity, the test specimen was modeled using 3D finite element. Stress and strain

concentrations for stiffener tapers of 45°, 60°, and 75° were calculated. The axial strain concentration was of the order of 4.6 for both braided and woven panels. The axial, transverse, and shear stress concentrations, respectively, were 4.10, 0.39, and 0.80 for braided panels (45° taper) and were 3.81, 0.27, and 0.50 for woven panels. Due to large rotation of the specimen, local strain calculation required a large-deformation analysis. Good correlation was obtained between the test response of the specimens and analysis.

The study has shown that the braided construction of the stiffener/panel interface can avoid the premature failure mode characterized by stiffener separation. This was not the case for woven construction as the panels tested failed by stiffener separation at roughly 25% of their tensile strength capability. Better manufacturing and through-the-thickness reinforcement may avoid experiencing this limiting failure mode.

1. INTRODUCTION.

Advances made in laminated, fiber-reinforced composites have proved that they are stronger, stiffer, and lighter than conventional metallic materials for a number of applications including aerospace structures, sports equipment, and transportation structures. Because the fiber-reinforced composites are used to replace metallic counterparts, from both the point of view of manufacturing and construction and design, their full potential has not been realized. Instead, the application of this material has been restricted by its low interlaminar strength. A major deciding factor in today's aircraft industries is the cost. Laminated, fiber-reinforced composites are not cost competitive. Therefore, efforts have been made to develop cheaper, better, and faster manufacturing processes. Since textile preform composites are amenable to net shape manufacturing, they will have fewer parts, few or no joints, less material scrap, and better interlaminar properties.

A number of studies have been undertaken to evaluate the potential of textile composites [1], examining such factors as the manufacturability and engineering mechanics issues. In this report an application of textile preform composites to aircraft stiffened panels is demonstrated.

Stiffened panels are widely used in airframe constructions. In stiffened panels, stiffeners are terminated at numerous locations to accommodate cross members or cutouts. These terminations or cutouts are sites of geometric discontinuities that induce high interlaminar stresses and stress gradients. High interlaminar stresses result in stiffener disbonding from the skin. Northrop Grumman Corporation, under a Federal Aviation Administration contract, investigated the structural integrity of laminated composite panels with stiffener discontinuity under tension, compression, and cyclic loading. [2] This study had two distinct objectives. The first was to study the structural integrity and failure modes of typical stiffened panels. The second was to formulate static strength and fatigue life certification procedures based on strength and life data generated by testing appropriately designed stiffened panels with stiffener discontinuity. This study found that in laminated, stiffened panels the failure initiated at the stiffener terminations both under static and fatigue loading conditions. As expected, high interlaminar stresses were responsible for this failure initiation.

The present study was focused on evaluation of stiffener discontinuity in integrally braided and woven composite panels. In textile preform panels, delamination failures, which usually occur in laminated composites, may no longer exist because of the integral fiber construction. However, there may be other matrix related failures. The panel configuration used in this study was similar to that used in the Northrop Grumman program.

The objectives of this study were to (1) design test specimens; (2) perform finite element analysis of test specimens and compare with the test results; (3) perform static tension tests and evaluate the failure modes and stresses in discontinuous stiffened three-dimensional (3D) braided and orthogonal woven composite panels; and (4) perform fatigue tests, evaluate damage accumulation, and determine the residual strength.

The Northrop Grumman test panel is described in section 2. The North Carolina A&T State University's (NC A&T) two-bladed stiffened panel and material system are described in section 3. In situ properties of the materials are measured in section 4. These properties will be used in finite element analysis. In section 5, the textile composite panels were designed to meet a stress-strain invariant condition. The detailed 3D stress-strain behavior was calculated for all test panels from a large-deformation, finite element analysis. In section 6, the static tension test results are presented and fatigue results are presented in section 7. Finally, results are summarized and compared with the laminated panel data in section 8.

2. NORTHROP GRUMMAN PANEL.

The test panel used in the Northrop Grumman study [2] is shown in figure 1. This test panel was designed to have the same overall cross-sectional dimensions as panels used in the aircraft industry such as the stiffened panels in the Boeing B-737 horizontal stabilizer. It consisted of a soft skin with an I-section stiffener. The flange thickness in the notched section of the panel was increased to 0.146 inch (3.7 mm) with a $[\pm 45/90/\pm 45/90/0/\pm 45/90_2/\pm 45/0]_s$ layup. The I-section stiffener had a $[\pm 45]_s$ layup. There was also a stiffener cap with a $[\underline{45}/0_6/\underline{45}]$ layup where $\underline{45}$ signifies biwoven layers. The criteria used in the design of these panel specimens were (a) the stiffener should have a minimum 1 inch length in which the stresses should remain constant and (b) the stiffener should carry at least 20% of the axial load on the panel. The panel skin was fabricated from AS4/3501-6 unidirectional tape and the stiffener was fabricated from AS4/3501-6 graphite epoxy woven fabric. The tests performed on this panel specimen included static tension and compression tests and compression-compression fatigue tests.

3. NC A&T TWO-BLADED STIFFENED PANEL.

3.1 PANEL GEOMETRY.

The NC A&T test panels were machined from the two-bladed integrally braided and woven panels, shown in figure 2, that were originally fabricated by the Mars Mission Research Center (a joint NC State and NC A&T State Universities program). The two-bladed panels were 457 mm (18 in.) long, 165 mm (6.5 in.) wide, the nominal depth of the blades was 19 mm (3/4 in.), and stiffener spacing was 89 mm (3.5 in). Two stiffened panel test specimens and several in situ test specimens were extracted from each of these two-bladed panels. The specimen layouts within the panels are shown in figures 3 and 4 for braided and woven composites, respectively. All the in situ property test specimens were extracted from the middle of the panels. The two outer sections with the stiffeners were used for the discontinuous stiffener panel study.

3.2 MATERIAL SYSTEM.

All panels were made of BASF G30-500 graphite fibers and Dow Chemical Tactix 123 matrix. Three-dimensional integral braiding and weaving technology was used in manufacturing the panels with stiffeners. The fabric architecture of the braid was designated by ($0°/\pm 17°$) with 46% $0°$ axials; whereas the 3D orthogonal woven fabric architecture was ($0°/90°/90°$) with 50% $0°$ axials. In woven fabric designation, the three numbers designate tow orientations in the x-, y-, and z-directions. The x-direction is the length direction for both braided and woven panels. The

volume percent of tows in the three directions for the braided composite used here is 46, 27, and 27. The volume percent of tows in woven preform is 50, 25, and 25 in the x-, y-, and z-directions. The fiber patterns revealed by sections of the panel in different orientations are shown in figures 5 and 6. The average fiber volume fractions of the braided and woven composites were 0.38 and 0.44, [3] respectively. Tension, shear, and compression test coupons extracted from the two-bladed panels were used to measure the in situ elastic properties of the panel material.

4. MEASUREMENT OF IN SITU PROPERTIES.

The mechanical properties of the braided and woven composite materials used in this study were not readily available. Further, there is likely to be some panel to panel variations in the mechanical properties. Since these properties are essential to predict the structural behavior of test panels, tests were performed to determine the tension, compression, and shear in situ properties of the panels. Tension and shear properties are presented here and the compression properties were previously reported in reference 3. Tension and shear test specimens were extracted from the two-bladed stiffened panels and they were tested. The other 3D properties required for the finite element analysis were estimated.

4.1 TENSION TEST.

The geometrical configuration of the tension test specimen is shown in figure 7. Because of the limited availability of material for these in situ tests, the length and width of the tensile specimens were selected to be 150 mm (6 in.) and 25 mm (1 in.), respectively. Although these specimens are shorter than the laminated test specimens proposed in the ASTM D 3039 test standard, they are of sufficient length to give accurate data. Specimens' grip ends were reinforced with 50- x 25- x 6.25-mm (2- x 1- x 0.125-in.) crossply glass/epoxy tabs with 45° end taper. The front and back surfaces of the tension specimens were instrumented with longitudinal and transverse strain gages having a 6.25- x 6.25-mm (0.25- x 0.25-in.) grid area. Three braided and five woven composite specimens were prepared and tested.

These specimens were tested under load control at a rate of 22 kN (5000 lb) per minute until failure. The load, displacement, and strain were recorded using a computerized data acquisition system. The average of the front and back surface strains was used in determining the stress-strain response, axial modulus, and the Poisson's ratio calculations.

The stress-strain responses of the braided and woven tension specimens are shown in figures 8 and 9, respectively. The failure mode for these specimens is shown in figures 10 and 11. In the case of the braided panels, the failure occurred within the gage length for all three specimens. The influence of the $\pm 17^\circ$ orientation of the braided tows near the specimen edge was indicated by the amount of those tows that had pulled out instead of fracturing. Therefore, the true strength of braided specimens may be larger than the measured values due to the edge effects. Five woven composite specimens were tested in tension; two failed in the tab region and the tabs debonded in three specimens before the specimen failure (see figure 11). The tensile modulus and strength of the braided and woven composite panels are listed in table 1. The average axial

modulus of braided and woven composites were 57.97 GPa and 59.40 GPa, respectively. The corresponding standard deviations were 8.0 GPa and 12.2 GPa, respectively. The average tensile strengths of braided and woven composites were 383.4 MPa and 674.5 MPa, respectively. The corresponding standard deviations are 59.2 MPa and 47.4 MPa, respectively. The average Poisson's ratios (ν_{xy}) of braided and woven composites were 0.88 and 0.05, respectively, which is reasonable for these fabric architectures. The corresponding standard deviations were 0.10 and 0.003, respectively.

4.2 SHEAR TESTS.

The shear properties were determined from specimens fabricated with dimensions in accordance with the ASTM standard D 5379. The geometry of the shear specimen is shown in figure 12. One surface at the notch in each specimen was instrumented with special shear strain gages (Micro-Measurement N2A-08-C032A-500-SP61) for measuring the shear strain as shown in figure 12. Four braided and three woven composite specimens were prepared and tested.

These specimens were loaded using the Iosipescu test fixture shown in figure 13. They were loaded under stroke control at a rate of 1.25 mm/min. The load, displacement, and strain were recorded using a computerized data acquisition system. These specimens underwent large shear deflections at the notch. Because of this large deflection and the subsequent undesirable contact between the test fixture, the test was stopped before the final fracture of the specimens. From the strain gage output, the shear stress-strain response and the shear modulus were determined.

The shear stress-strain responses of the braided and woven specimens are shown in figures 14 and 15, respectively. The shear modulus was calculated from the average slope of the shear stress-strain curve between the strains 1000 $\mu\varepsilon$ and 4000 $\mu\varepsilon$. The shear yield strength was estimated based on the 0.2% offset method. The shear properties for these materials are given in table 2. The shear moduli for the braided and woven panels were 5.39 GPa and 2.51 GPa, respectively, and the corresponding standard deviations were 0.29 GPa and 0.30 GPa, respectively. The shear yield strengths for the braided and woven composites were 68.0 MPa and 25.6 MPa, respectively, and the corresponding standard deviations were 14.8 MPa and 1.1 MPa, respectively.

4.3 THREE-DIMENSIONAL ELASTIC PROPERTIES.

The elastic properties of the panels were required for the finite element analysis. Longitudinal and shear moduli and the major Poisson's ratio were measured. The remaining six properties were calculated from the fabric architecture and fiber volume fractions using the TEXCAD3D code. [4] Properties calculated for braided (B3A) and woven (W3B) panels are listed in table 3.

5. DESIGN AND ANALYSIS OF TEST PANELS.

5.1 DESIGN OF TEST PANEL.

The proposed test panel configuration is similar to the laminated composite panel that was used by Northrop Grumman Corporation. [2] However, the NC A&T test panel had a blade stiffener compared to the I-section stiffener used in the Northrop Grumman test panel. The stiffener in the NC A&T panel was notched at the midspan and at the ends. The end notch was introduced to bond the loading tabs. A schematic diagram of the notched test specimen is shown in figure 16. The nominal length and width of the test panels were 457 mm (18 in.) and 50.8 mm (2 in.), respectively. There were four unknown geometric parameters in this test panel, the constant strain region in the notched ($2l_n$) and unnotched sections (l_s), the notch taper angle (θ), and the grip length (l_g). The grip length was selected based on the maximum load and the friction factor of the loading grips. For an estimated maximum load of 200 MPa (45 kips), a grip length l_g of 64 mm (2.5 in.) was found to be adequate. Three taper angles, 45°, 60°, and 75° were evaluated by finite element analysis and finally the taper angle of 45° was chosen. The other two parameters, l_s and l_n, were established by finite element analysis. Since achieving uniform strain across the cross section is almost impossible in a notched specimen, an invariant strain criterion was used. Strain invariance means that the strain field across the specimen would remain constant over a certain length of the specimen. A requirement of strain invariance over at least 25 mm (1 inch) length of the stiffener as well as the notched section was used to establish l_s and l_n. The following dimensions were chosen for the panels: the notch root radius R_2 = 32 mm (1/8 in.), l_g = 64 mm (2.5in.), R_1 = 25.4 mm (1 in.), and the specimen length L = 457 mm (18 in.). The other geometric parameters, i.e., height of the stiffener h_s, the thickness of the flange t_p, the thickness of the stiffener t_s, were different from specimen to specimen. Stiffener depth, h_n, at the midsection was 3.2 mm (0.125 in.). The loading ends were reinforced with 15.9-mm-thick crossply fiber glass tabs.

5.2 FINITE ELEMENT ANALYSIS OF TEST PANEL.

5.2.1 Finite Element Model.

A finite element model of one-quarter of the test specimen is shown in figure 17. This model had 12,740 nodes and 2575, 20-noded isoparametric, solid elements with anisotropic material properties. The finite element mesh at the notch root region was refined to capture the stress and strain concentrations. Symmetric boundary conditions were imposed on the z = 0 and x = l/2 planes. A uniform displacement u_x was imposed on the specimen at x = 0. Since the friction grips do not allow the tabbed length of the specimen to rotate, an equivalent condition was simulated analytically by restraining y-direction displacement of the tabs. A preliminary calculation showed that the tabs could be compressed by nearly 0.05 mm (0.002 in.) in the y-direction under the maximum axial load on the specimen. Therefore, one-half of the y-displacement was imposed on the top and bottom tab surfaces over the gripped area to provide rotational constraint. The material properties given in table 3 were used for modeling both the flange and stiffener of the panel. The finite element model was built such that the model dimensions and discretization can be varied depending on the values of l_n, l_s, and θ. A linear elastic analysis was conducted to establish the stress invariant region in the test panel. A large-

displacement, nonlinear analysis was conducted to account for the large rotation of the test specimen. The commercial finite element analysis code ANSYS [5] was used in all the analyses.

5.2.2 Test Panel Design.

A linear stress analysis of both braided and woven composite panels was conducted for various values of stiffened (l_s) and notched (l_n) lengths. The taper angle was kept at 45°. As mentioned previously, it was impossible to get uniform (pure membrane condition) stress all across the specimen. Therefore, the invariance of the axial strain (ε_x) field across the specimen depth was used as a design criterion. Figure 18 shows the variation of ε_x at the z = 0 plane at various depth (y/d_w) locations. Note that strains are plotted over the unnotched length of the stiffener. Strain at all y/d_w locations was almost constant (less than 5% variation) for s = 25 to 75 mm (i.e., for a length of about 50 mm). The length over which there is less than a 5% variation of ε_x was assumed to be the invariant length. The invariant strain region for the woven composite panel was about 65 mm. An examination of the invariant lengths in the stiffened and unstiffened sections of the braided and woven panels found them either equal or greater than those in Northrop Grumman studies. Therefore, the proposed configuration for the braided and woven composite panels is satisfactory to produce stress states similar to that of the laminated composite panel. [2]

5.2.3 Linear Analysis Results.

Figure 19 shows the deformed mesh of a braided composite panel. To the quarter model's deformed mesh, a mirror image was added to show the complete panel's deformation. The deformed shape indicates that (1) the maximum bending strain occurs at the top surface in the midsection of the panel, (2) the peel (s_y) and shear (τ_{xy}) stresses are concentrated at the notch root of the stiffener, and (3) reversed bending occurs in the stiffened panel. Stress and strain concentration factors at the notch root of both braided and woven panels are listed in table 4. All stresses were normalized by the average stress (σ_0) at the midsection of the panel. The variation of the axial stress concentration factor (K_x) as a function of the angle θ showed no definitive trend. The stress concentration factor (K_x) of braided panels for θ values of 45° and 75° were 4.10 and 3.83, respectively. For woven panels K_x ranged from 3.87 to 3.96. Therefore a taper angle of 45° was selected in the test program. The peel (K_y) and shear (K_{xy}) stress concentration factors were very high for braided composites, about 39% and 80% of the axial stress, respectively. For woven specimens they were 27% and 50%, respectively. Since both laminated as well as textile preform composites are weak in the transverse and shear strengths, these high stress values, particularly peel stresses, should initiate peel failure. Because the braided composites have interlocked fiber preform architecture, failure initiated either as peeling or shear would not propagate further. However, the 3D orthogonal woven composites, which are weak in shear, could fail by the longitudinal shearing of the stiffener. Table 4 also gives the axial strain concentration (K_{ε_x}) at the notch root, which varies from 4.45 to 4.77 for braids and from 4.56 to 4.68 for weaves. The high strain concentration at the notch again indicates that failure could initiate at the notch root. The variation of the peel and shear stress distribution for a taper angle of 45° from the notch root into the stiffener is shown in figure 20. Stress distributions for all other taper angles had nearly the same trend as shown in figure 20.

5.2.4 Large-Deformation Analysis.

The deformed shape (see figure 19) of the test panel shows considerable rotation at various sections of the panel. To evaluate the effect of rotation on local stresses and strains, a large-deformation analysis was conducted. The ANSYS code [5] uses the derivatives of the displacements as the nonlinear terms in the formulation. The analysis was conducted by increments of remote displacements. Stresses and strains at each of the incremental displacements were calculated. The panel end load and displacement response of the braided and woven composite panel are shown in figure 21. The linear solution is represented by dashed lines and the nonlinear solution by solid lines. The difference between linear and nonlinear results is very small (less than 2%). The global response of the panels is almost linear.

Figure 22 shows the strain gage locations used in the test panels. Strains in the top and bottom surfaces of the flange were used to evaluate nonlinearities and to compare with test data. The variation of the top surface strains at g_1 and g_5 locations (the stiffener center and notch center locations) as a function of the average axial stress (σ_0) for the braided composite panel is shown in figure 23. Dashed lines represent the linear solution and solid lines are nonlinear solutions. For a given applied stress at g_1 (the stiffener center location) the strain determined from the nonlinear analysis is larger than the one from linear analysis, whereas at g_5 (the notch center location) the strain determined using nonlinear analysis is less than the one from linear analysis. The difference between linear and nonlinear strain is large enough to warrant a large-deformation analysis to calculate accurate stresses. The woven composite panel results are similar to the trend of braided panels.

Figure 24 shows the variation of the membrane $\{(\varepsilon_t + \varepsilon_b)/2\}$ and bending $\{|(\varepsilon_t - \varepsilon_b)|/2\}$ strains as a function of the average stress, σ_0. Membrane strains at g_1 (the stiffener center location) and g_5 (the notch center location) were almost identical, and they vary linearly with σ_0. However, the bending strains display an asymptotic variation. The bending strain at g_5 (at the notch center location) is twice that of g_1 (the stiffener center location). Therefore, the nonlinearity is due to the nonlinear variation of bending stress with load. The response of woven specimens was also similar.

Load flow in flange and stiffener were analyzed. The load carried by the stiffener was about 14% and 13% of the total load for braided and woven specimens, respectively.

6. STATIC TENSION TESTS.

Static tension tests were conducted on five braided composite panels and five woven composite panels. The panels were strain gaged as shown in figure 25. A photograph of a woven specimen is shown in figure 26. There were small differences in the flange and stiffener thicknesses among the different panels which resulted in differences in total cross-sectional areas. The actual cross-sectional areas of these specimens in the notched region are listed in table 5.

6.1 INSTRUMENTATION AND TEST PROCEDURE.

All panel specimens were instrumented with strain gages with a 12.3- x 4.6-mm active grid area. Figure 25 shows the individual strain gage locations on the specimen surfaces. The same numbering scheme for the strain gages was maintained for all the panel specimens. However, not all the gages were present in all specimens. Gages g_4 and g_{10} were back to back on the specimen. Other back-to-back strain gage pairs were g_1 and g_{12}, g_6 and g_{13}, g_5 and g_{14}, and g_9 and g_{15}. The strain gages were connected to a 20-channel data acquisition system. In addition, the region around the notch, where high peel and shear strains are expected, was coated with a thin, uniform layer of white typewriter correction fluid. This layer served as brittle coating, indicating regions of severe strains by cracking. Failure initiation in these regions was monitored during the tests. Panels were tested in a 50-kips MTS test machine equipped with hydraulic grips. A photograph of a typical panel specimen is shown in figure 26. The experimental setup is shown in figure 27. Some panels were tested under displacement control (0.5 mm/min) while others were tested under load control (22.24 kN/min). During the test the load, stroke displacement, and strains were continuously recorded. Regions likely to fail (notch root) were continuously monitored. The loads at initiation of failure and final fracture were recorded. All the final fracture loads are listed in table 5.

6.2 TEST RESULTS.

6.2.1 Load-Displacement Response.

The load-displacement responses of three braided and three woven specimens are shown in figures 28 and 29. The load-displacement response of braided and woven composite panels was initially linear and at higher loads became nonlinear. The nonlinearity was due to a number of microscopic failures initiating and progressing in the specimen.

6.2.1.1 Braided Composite Panels.

The load-displacement responses of all braided panels were similar, but the B1B response was lower, as shown in figure 28. Most of the braided specimens showed the first failure around the notch root of the stiffener. As the load increased, the number of cracks increased both at the notch root and all along the notch section. Finally, specimens failed in net section tensile failure. Figure 30 shows a photograph of the failure mode.

6.2.1.2 Woven Composite Panels.

The load-displacement responses of the woven panels W2A and W2B were similar (see figure 29), but panel W3B appeared to be stiffer which is consistent with the coupon data of table 1. In these panels, failure initiated due to high shear stresses either at the notch root or at the stiffener-flange interface at the end of the specimen and propagated to partial or full separation of the stiffener from the flange (see figure 31). In contrast to braided panels, all woven panels emitted a considerable amount of audible sounds throughout the loading cycle. In the case specimen W2A, the shear crack between the stiffener and flange that initiated at the specimen ends was observed to have traversed beyond the tabs and could be seen on the white

coating at a load level of 36 kN (20% of maximum load). This crack grew along the specimen length as the load was increased until the final separation of the stiffener from the panel. After the stiffener separated, the panel response was like a uniaxial specimen. For specimens W2B and W3B, the shear crack started near the notch root. For specimen W2B these shear cracks initiated at a load level of 58 kN (28% of maximum load) and by the time the load reached 156 kN (76% of the maximum load) the shear crack had extended by nearly 50 mm. The final fracture, however, was a net section tensile failure for all the woven composite panels. The failure occurred away from the notched area in all woven specimens and the final failure was due to a weak spot created by the shear crack between the flange and stiffener. Because initial failure was stiffener separation, the woven panels behaved similarly to traditional construction panels. [2]

6.2.1.3 Comparison of Braided and Woven Panel Responses.

Table 5 lists the fracture load and the fracture stress (based on the cross-sectional area at the midsection of the specimen) of all the tested panels. The average fracture strength of braided composite panels is 433.7 MPa, with a ±17% variation. In comparison, the strength of braided composite coupons (see table 1) was 383.4 MPa; i.e., the strength determined from the panel tests was 13% higher than the strength determined from coupons for braided material. This difference is primarily due to edge effect caused by ±17° braid tows in coupons. The average fracture strength of the woven panels is 581.8 MPa with +7% and -14% variation.

The average axial elastic moduli of the braided and woven panels was determined from the average stress applied at the notch section and the membrane strain determined from the strain gage data described in the following section. The average axial elastic modulus of braided composite material determined from the panel tests was 80.36 GPa with a +15% and -12% variation. In comparison, the average modulus determined from the braided composite test coupons was 57.97 GPa; i.e., the modulus determined from panel tests was 39% higher than from the coupon tests for braided material. The average axial elastic modulus of woven composite material determined from the panel tests was 71.70 GPa with a +22% and -24% variation. In comparison, the average modulus determined from the woven composite test coupons was 59.40 GPa; i.e., the modulus determined from panel tests was 21% higher than from the coupon tests for woven material. The differences seen in the stiffness properties between the panels and the coupons can be attributed mainly to material variabilities within the panels due to process conditions.

6.2.2 Strain Response.

Typical load-strain responses of the braided and woven composite specimens are presented in this section. For completeness, the results corresponding to the rest of the panels are included in appendix A. These plots include (a) the specimen surface strain response at various strain gage locations and (b) the bending and membrane strains at the midplane of the flange in the notched section as well as in the middle of the stiffened region.

6.2.2.1 Braided Composite Panels.

Response from the braided composite panel B1B was selected as typical. Strain gage responses of the other braided panels were similar and those results are included in appendix A. Specimen B1B was instrumented with 11 strain gages. Gages g_1, g_4, g_7, and g_9 were in geometrically equivalent positions in the lengthwise center of the stiffened region (see figure 25). Among these gages, g_1, g_4, and g_9 had similar strain responses (see figure 32). But the strain from gage g_7 was about 20% higher than from gages g_1, g_4, and g_9. Gages g_3 and g_8 were positioned on the two stiffener segments with their centerline at a distance of 5.1 mm from the flange-stiffener corner. The strains indicated by these gages were about 65% of the strain recorded by g_1 (flange).

The strains in the gages located symmetrically at the notched section, namely, gages g_5 and g_6, had identical strain readings until failure. At a load level of 110 kN, gages g_5 and g_6 measured a large increase in the strain indicative of local damage growth. The specimen failed at the center of the notched region with a significant amount of $\pm 17^\circ$ fiber pullout, as shown in figure 30. The pullout length was highest for those fibers which were cut during the machining of the specimens at the flange edges and at the stiffener notch region. The final failure appears to have initiated from the notched surface of the stiffener in a manner similar to the fiber pullout seen in the in situ tensile specimens shown in figure 10. The tensile strength of the panel based on the cross-sectional area at the notched region was 368.5 MPa.

The flange midplane membrane and the bending strain components are shown in figure 33. The membrane components of the strains at the centers of the notched region and the stiffened region are similar. But the bending strains at the corresponding locations have opposite signs and are indicative of reversed bending at these locations. The bending component of the strain shows a higher level of nonlinearity than the membrane components which are fairly linear. The difference between the two membrane strains and the cross-sectional areas (multiplied by the applied load) would be a measure of load carried by the stiffener. The stiffener load was estimated to be about 15% of the total load.

6.2.2.2 Comparison of the Membrane and Bending Response of Braided Panels.

The bending and membrane strain components in the notched region of the braided composite panels B1B, B3A, and B3B are shown in figure 34. The corresponding plots for the stiffened region are shown in figure 35. The responses of composite panels B3A and B3B match closely. But composite panel B1B shows higher levels of strain. It may be noted that this specimen also had a significantly lower strength (368.5 MPa).

6.2.2.3 Woven Composite Panels.

The results from panel W2A are discussed in this section. The strain response of other woven panels were similar and they are included in appendix A. The strains measured at various locations of woven composite panel W2A are shown in figure 36. Gages g_1, g_4, g_7, and g_9, located at geometrically equivalent positions, had similar strain responses. Gages g_3 and g_8, located on the stiffener at a distance of 5.1 mm from the flange-stiffener corner, measured a strain that was approximately 55% of the strain measured by g_1. Gages g_5 and g_6, symmetrically

located at the notch section of the flange, had similar strains. The effect of the growing crack between the flange and the stiffener could be seen in the nonlinear behavior of strains from gages g_3 and g_8 located on the flange. For this specimen, the tabs debonded at a load level of 179.3 kN. The tensile stress based on the notch cross section at this load level was 565.1 MPa.

The flange midplane membrane and bending strains are shown in figure 37. Strains were not measured at specimen failure because of strain gage failure. As in the case of the braided composite panel B1B, the membrane components at the notch region and the stiffener region are similar, but the bending components have opposite signs. Further, the membrane components are linear while the bending components are nonlinear. The load carried by the stiffener could be estimated from the difference in the membrane components of strain at the notch and stiffener regions, and the load carried by the stiffener was about 10% of the total load.

6.2.2.4 Comparison of Membrane and Bending Response of Woven Panels.

The bending and the membrane strain components at the notched region of the woven composite panels W2A, W2B, and W3B are shown in figure 38. Similar plots for the stiffened region for specimens W2A and W3B are shown in figure 39. Specimen W2B was not strain gaged in the stiffened region. The membrane strain response of the woven composite panels W2A and W2B were similar, but woven composite panel W3B was stiffer. This is consistent with the overall behavior shown in figure 29 and the tensile coupon results of table 1. W3B failed in the grip area and the strength of this specimen, based on the notch section area, was 499.6 MPa.

6.3 COMPARISON OF TEST AND ANALYSIS RESULTS.

Figure 40 shows a comparison of the experimentally measured strains and the finite element predictions for the braided composite panel B3A at gage locations g_1 and g_5. The finite element results correspond to a large-deformation analysis of the panels. The panel stiffness determined for this panel from the strain gage readings at the notch section, as described in section 6.2.1, was used in the finite element analysis. Other mechanical properties used in the finite element analyses are shown in table 3. There was excellent agreement between the measured and the finite element strains at the stiffener center and at the notch locations for the braided composite panels. Similarly, figure 41 shows excellent agreement between the measured and the finite element strains at gage locations g_1 and g_5 for the woven composite panel W2A. As in the case of the braided specimen, the stiffness determined for this panel from the strain gage readings at the notch section was used in the finite element analysis. The results for other braided and woven panels agree reasonably well.

7. FATIGUE TESTS.

Tension-tension fatigue tests were conducted on braided and woven composite panels. The specimen configuration of fatigue specimens was the same as that used in static tests. Because of the limited number of specimens available, the tests were limited to one stress value (S_{max}=0.6 S_{ult}) with a stress ratio, R, of 0.1. (R is defined as the ratio of the lowest stress divided by the highest stress in a cycle.) The average S_{ult} values for the braided and woven composite panels were 433.7 MPa and 581.8 MPa, respectively. One braided and three woven composite panel

specimens were available for the fatigue evaluation. However, two of the woven panels were damaged due to test machine malfunction; hence the results from one braided and one woven specimen are reported. The damage accumulation was measured through the change in compliance of the specimen. Compliance was measured using an extensometer. Figure 42 shows the specimen configuration with extensometer attachment points.

7.1 TEST PROCEDURE.

The specimens were tested under constant amplitude cyclic load with a maximum tensile load of 60% of the average static strength. The maximum load P_{max} for the braided composite panel was 91.63 kN. For the woven composite panel, P_{max} was 107.20 kN. The R ratio was chosen as 0.1 for both the braided and woven composite panels. The loading frequency was 5 Hz for the initial 100,000 cycles of each test and was increased to 10 Hz for the remaining portion. The strain from the extensometer and the load were recorded using a data acquisition system. To start with, the specimen was subjected to a static load cycle (S_{max}=0.6 S_{ult}) to determine the initial compliance. This was followed by the fatigue loading under load control. The loading cycles were periodically interrupted to measure the specimen compliance. Compliance was calculated from the measurements of displacements at the minimum (S_{min}) and maximum (S_{max}) loads. These compliances were taken after 50, 100, 200, 300, 500, $1x10^3$, $2x10^3$, $3x10^3$, $5x10^3$, $10x10^3$, $15x10^3$, $25x10^3$, $40x10^3$, $50x10^3$, $100x10^3$, $200x10^3$, $300x10^3$, $400x10^3$, $500x10^3$, $600x10^3$, $700x10^3$, $800x10^3$, $900x10^3$, and $1x10^6$ loading cycles. The change in compliance was used as a measure of the damage accumulation in the specimen. Both the braided and woven specimens survived one million cycles of fatigue load after which the specimens were tested for residual strength.

7.2 TEST RESULTS.

7.2.1 Braided Specimen (B1A).

During the initial static loading cycle, audible sounds were heard at a load level of 22 kN (24% of S_{ult}). At a load level of 75 kN (49% of S_{ult}), a small crack was seen at the lower corner of the stiffener notch. After the static loading, the specimen was subjected to cyclic loading and compliance data were collected. As the loading cycles continued, the crack density at the notch root increased. After 34,000 cycles, additional cracks appeared in the top flange surface in the notch region. However, the stiffener-flange interface did not develop any further cracks, either due to peel or shear stresses, during the fatigue cycles. Figures 43 and 44 show variations of compliance and stiffness for this specimen. This specimen survived one million fatigue cycles and during this period the compliance increased by 9.3%. After the one million cycles of fatigue loading, the specimen was tested to obtain the static strength. The final failure occurred at a load level of 136.1 kN in the notch section. The residual strength was 384.2 MPa which was 88.6% of the average static strength of the braided panels.

7.2.2 Woven Specimen (W3A).

During the initial static loading cycle, a crack started at the notch root at a load level of 45 kN (25% of S_{ult}) and had grown to a length of 40 mm along the flange-stiffener interface at a load of

68 kN (38% of S_{ult}). The crack was caused by a shear failure in the notch root of the woven stiffener, which was an expected failure. As the number of loading cycles increased, the crack in orthogonally woven composite grew steadily. After about 500 fatigue cycles, the crack had progressed to a length that was nearly 75% of the stiffener lengths and there a was visible separation of the stiffener from the flange. Beyond this point, the panel behaved as a unidirectional fiber-reinforced laminate. The changes in the compliance and the stiffness for this specimen are shown in figures 45 and 46. For the woven panel, the changes in the compliance occurred rapidly in the beginning. The first 50% of change in the compliance took place in the first 1000 cycles, probably caused by loss of the stiffener. For one million cycles, the compliance increased by 7.8%. Even with the disbonded stiffener, the woven specimen survived one million fatigue cycles. This specimen was statically tested after the one million fatigue cycles, and failed at 171.2 kN. This corresponds to a residual strength of 528.7 MPa or 90.9% of the average static strength.

8. CONCLUDING REMARKS.

An experimental and finite element study was conducted to evaluate the structural integrity of integrally braided and woven textile composite stiffened panels with a stiffener discontinuity. Stress concentrations at the stiffener terminations were of concern.

A 3D finite element analysis was conducted to identify the regions of high stresses and design the test specimen with stiffener discontinuity. Good correlation was obtained between the test response of the specimens and analysis.

In braided composite specimens failure was initiated by peel stress resulting in local cracking until final fracture in net tension at an average strength of 433.7 MPa. Woven specimens failed by stiffener separation initiated by shear cracks at a stress of 162.7 MPa. These panels, however, were capable of sustaining higher loads because the load carried by the blade stiffener was only about 10% of the total load and eventually failed at an average strength of 581.8 MPa by net tension. Thus the behavior of the woven panels was similar to the conventional tape construction wherein the panels fail prematurely because of stiffener disbond.

One braided composite specimen and one woven composite specimen were tested under tension-tension fatigue with a stress value of $S_{max} = 0.6\ S_{ult}$ and a stress ratio of 0.1. The damage accumulation was measured through the compliance change of the specimen. Both the braided and the woven specimens survived one million fatigue cycles, but the woven panel lost its stiffener. The change in compliance for the braided and woven composite specimens in one million cycles was 9.27% and 7.83%, respectively. In the woven panel it was primarily due to stiffener loss. The residual strengths of braided and woven composite specimens were 384.2 MPa and 528.7 MPa, respectively, which is 88.6% and 90.9% of their corresponding average static strengths.

The study has shown that the braided construction of the stiffener/panel interface can avoid the premature failure mode characterized by stiffener separation. This was not the case for woven construction as the panels tested failed by stiffener separation at roughly 25% of their tensile

strength capability. Better manufacturing and through-the-thickness reinforcement may avoid experiencing this limiting failure mode. It is recommended that a woven panel especially designed against this failure mode be manufactured and tested to ascertain the validity of the tests performed under this program.

9. REFERENCES.

1. Poe, C. C. and Harris, C. E., (eds.), Mechanics of Textile Composites Conference, NASA CP-3311, Parts 1 and 2, October 1995.

2. Shah, C. H., Kan, H.P., and Mahler, M., "Certification Methodology for Stiffener Terminations," DOT/FAA/AR-95/10, April 1996.

3. Emehel, T. C. and Shivakumar, K. N., "Tow Collapse Model for Compression Strength of Textile Composites," Proc. of ASC 10th Technical Conference, Santa Monica, CA, October 18-20, 1995.

4. Branch, K., Shivakumar, K., and Naik, R., "TEXCAD 3D for 3D Triaxial Four Step Circular Braided Composites," Proc. of Symposium on Design and Manufacturing of Composites, 1996 IME Congress & Exposition, Atlanta, GA, November 1996.

5. DeSalvo, G. J. and Gorman, R. W., *ANSYS Engineering Analysis System User's Manual*, Version 4.4, Swanson Analysis Systems, Inc., Houston, PA, May 1989.

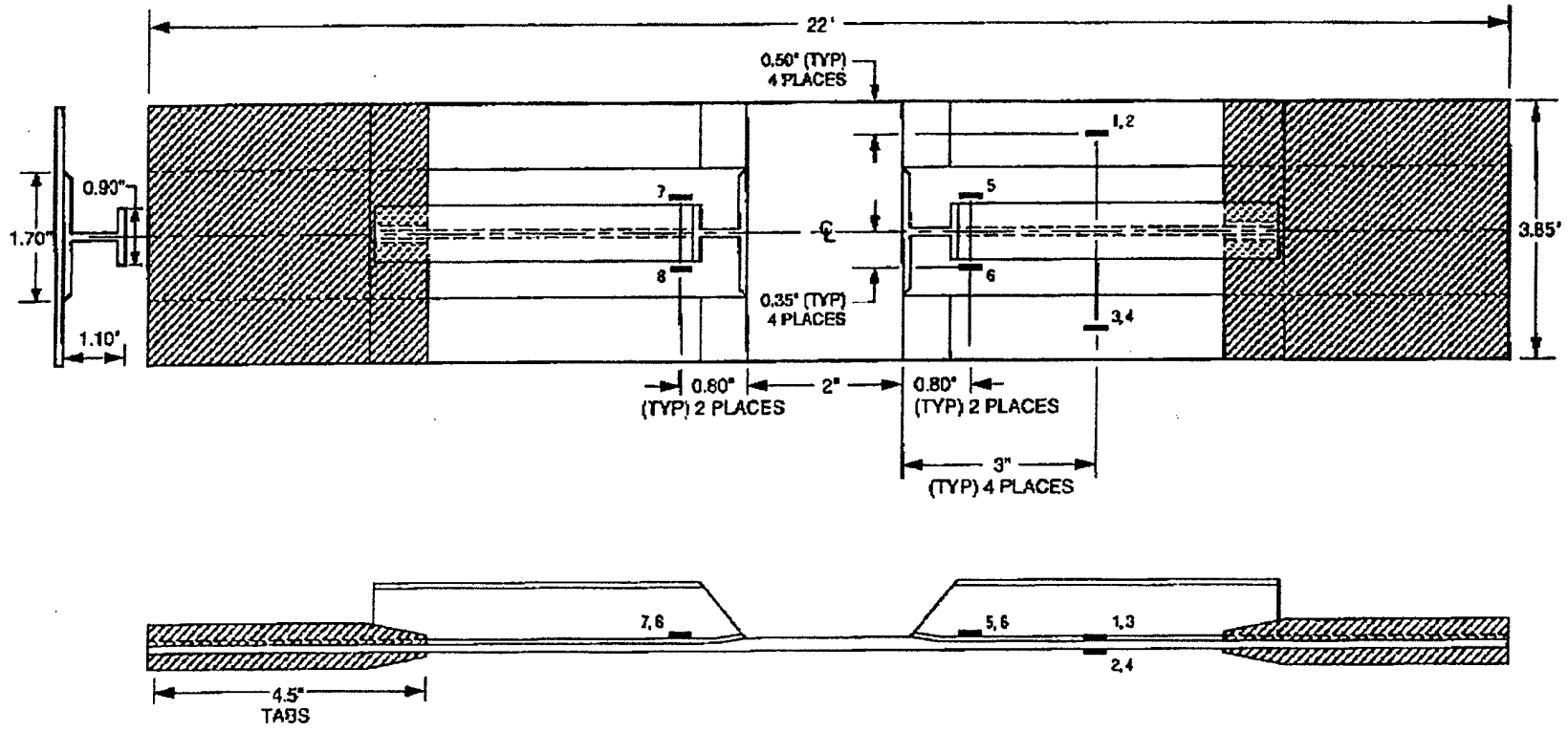

FIGURE 1. NORTHROP GRUMMAN STIFFENED PANEL TEST SPECIMEN

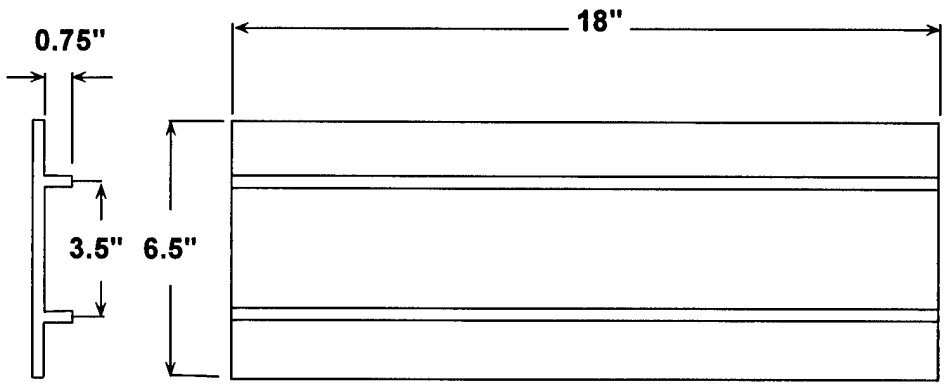

FIGURE 2. THE GEOMETRICAL DETAILS OF THE TWO-BLADED STIFFENED PANELS

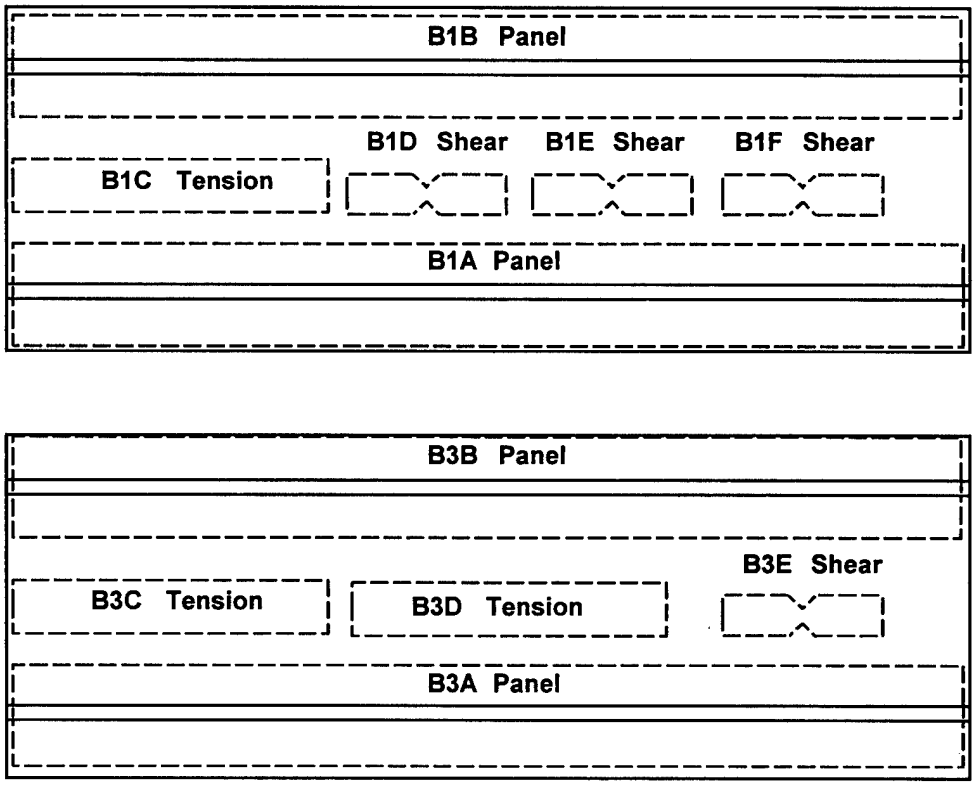

FIGURE 3. COUPON TEST AND PANEL TEST SPECIMEN LAYOUT ON THE TWO-BLADED STIFFENED BRAIDED PANEL

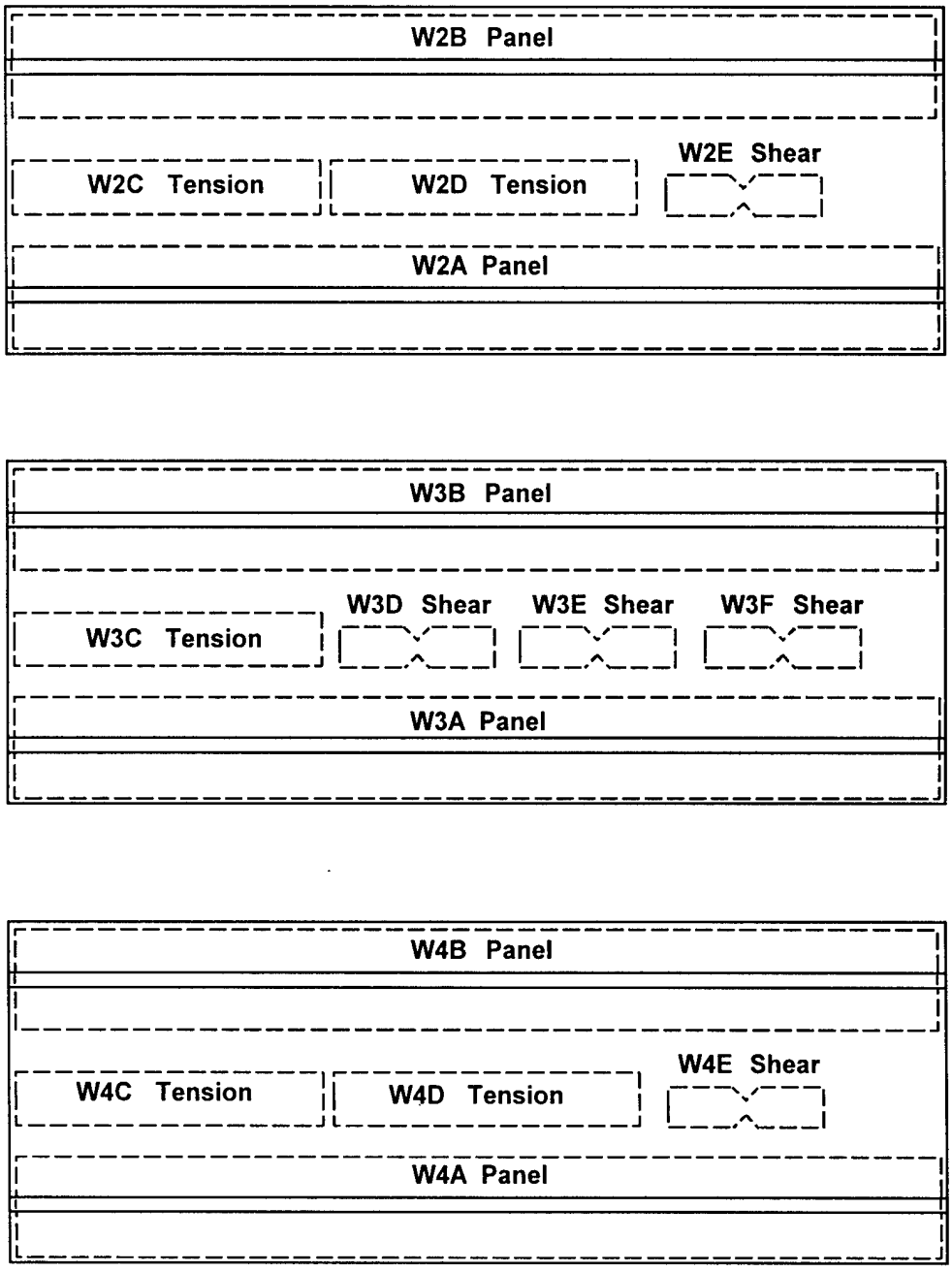

FIGURE 4. COUPON TEST AND PANEL TEST SPECIMEN LAYOUT ON THE TWO-BLADED STIFFENED WOVEN PANELS

(a) View of transverse section of panel (b) View of bottom surface of panel

FIGURE 5. FIBER ARCHITECTURE IN BRAIDED COMPOSITE PANEL

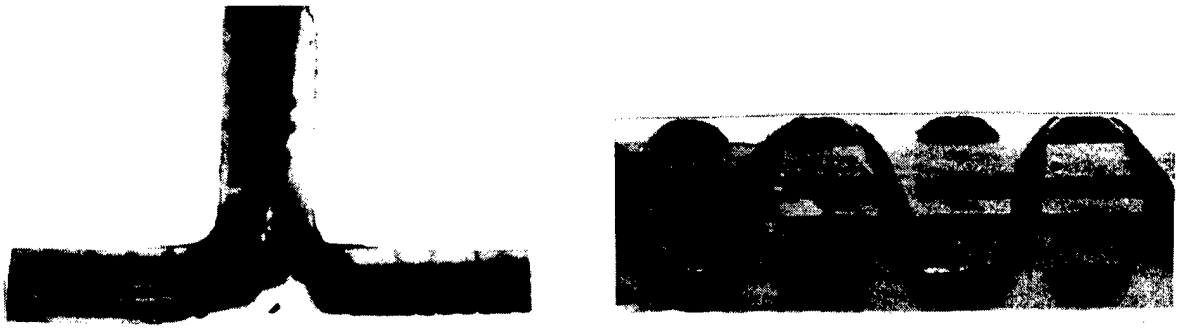

(a) View of transverse section of panel (b) View of longitudinal section of flange

FIGURE 6. FIBER ARCHITECTURE IN WOVEN COMPOSITE PANEL

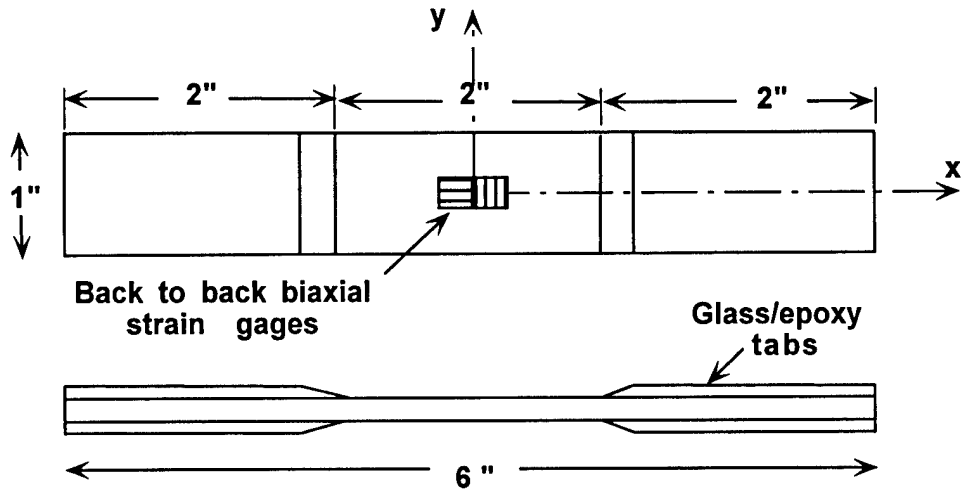

FIGURE 7. TENSION TEST SPECIMEN

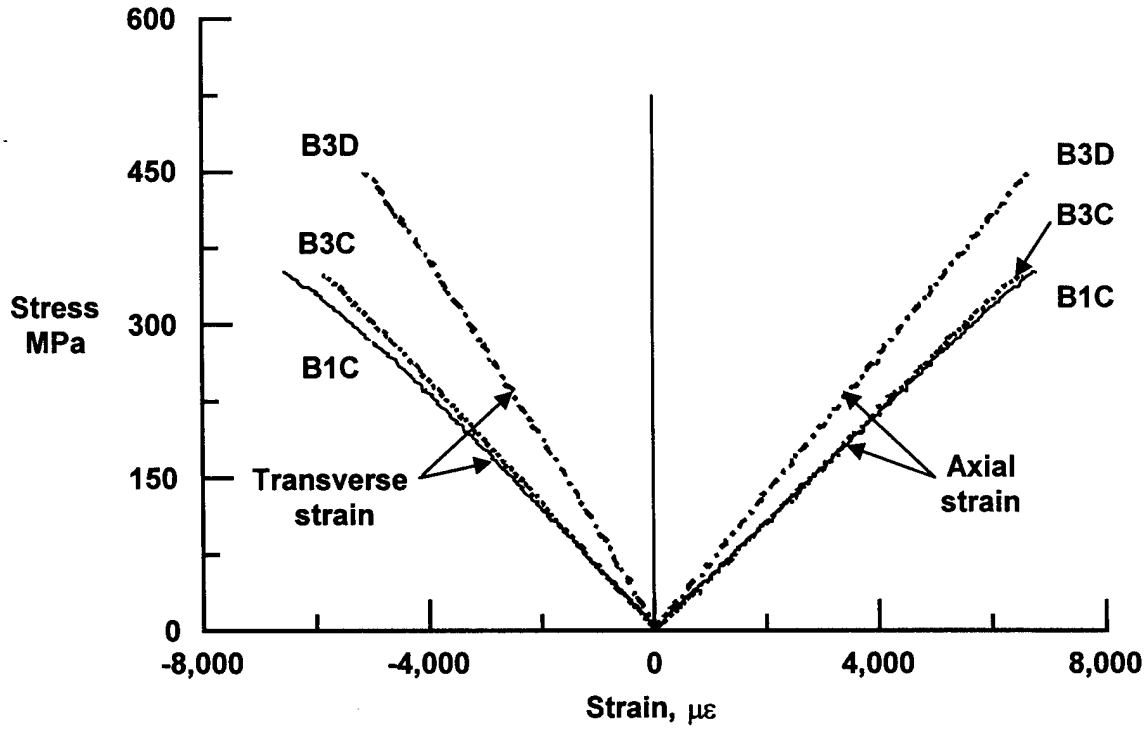

FIGURE 8. TENSILE STRESS-STRAIN RESPONSE OF BRAIDED COMPOSITE TEST COUPONS

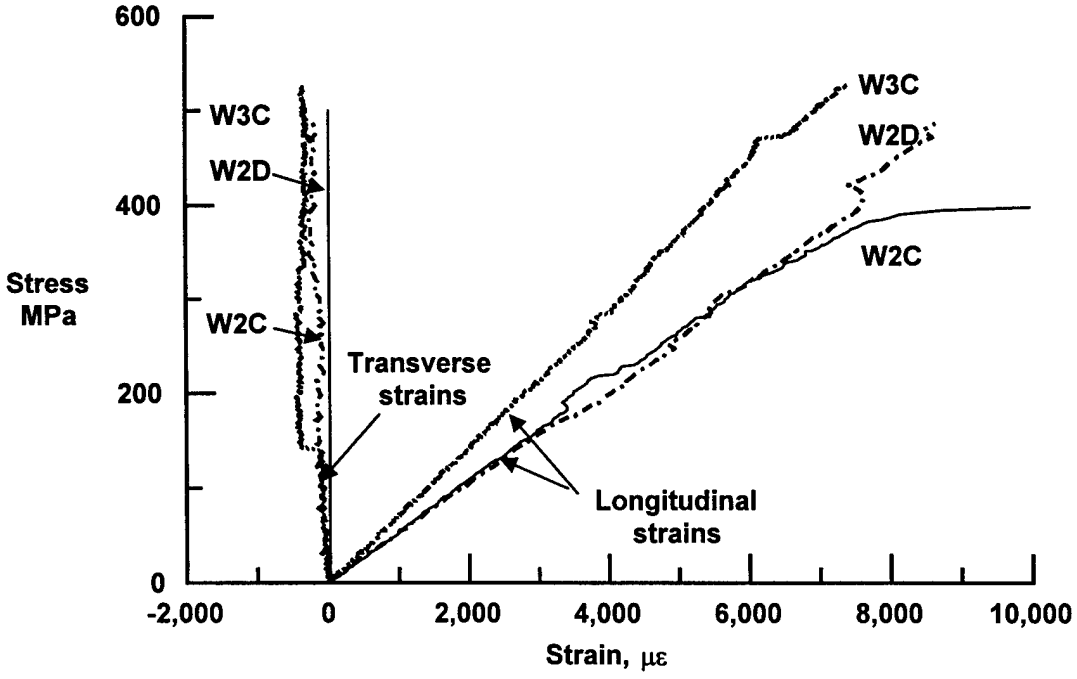

FIGURE 9. TENSILE STRESS-STRAIN RESPONSE OF WOVEN COMPOSITE TEST COUPONS

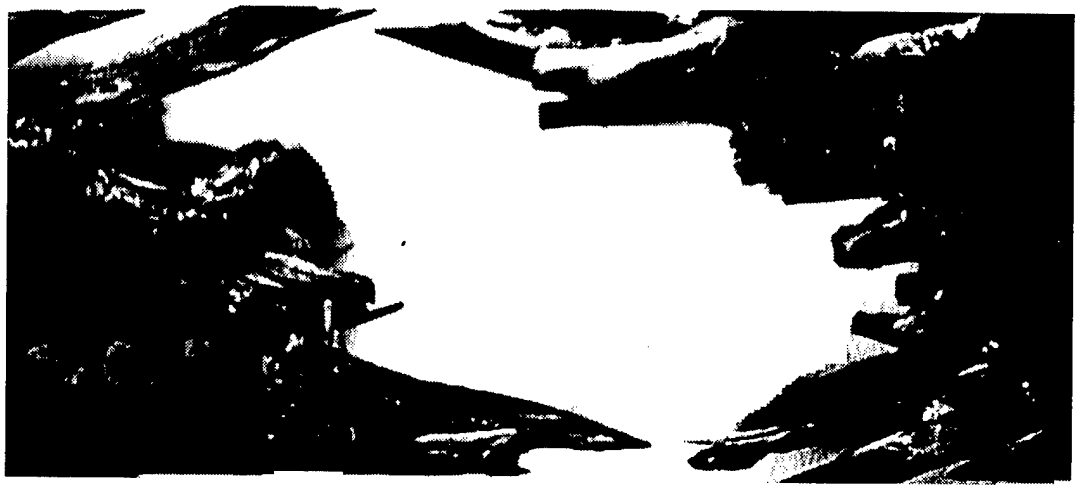

FIGURE 10. FAILURE MODE OF THE BRAIDED COMPOSITE SPECIMEN

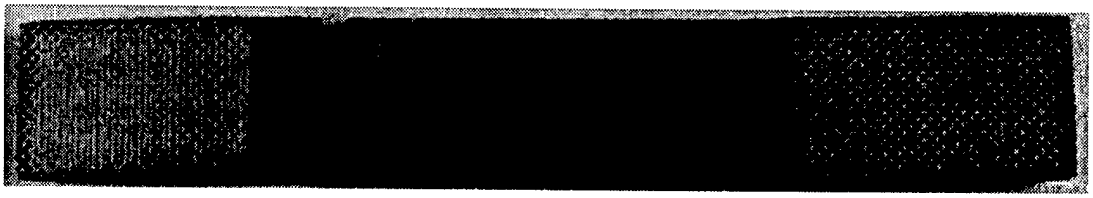

FIGURE 11. FAILURE MODE OF THE WOVEN COMPOSITE SPECIMEN

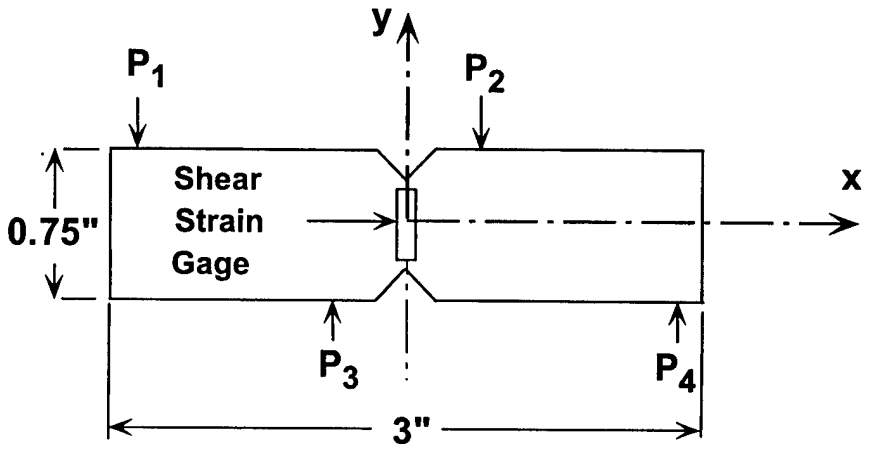

FIGURE 12. SHEAR TEST SPECIMENS

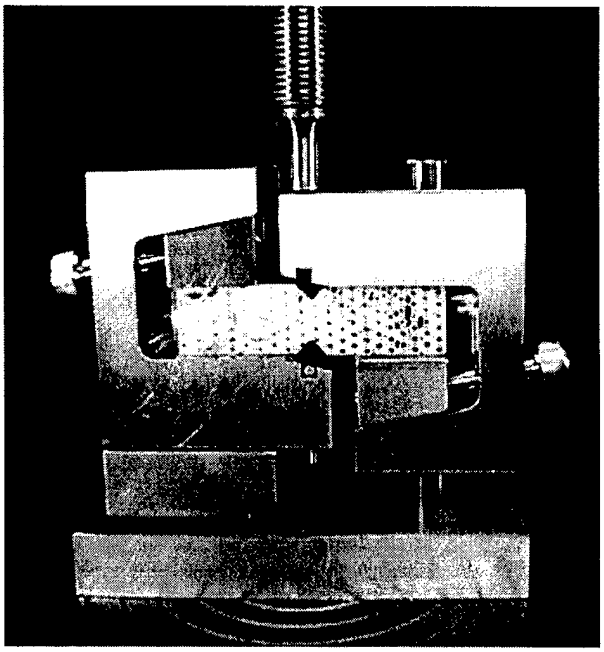

FIGURE 13. IOSIPESCU SHEAR TEST FIXTURE AND SPECIMEN

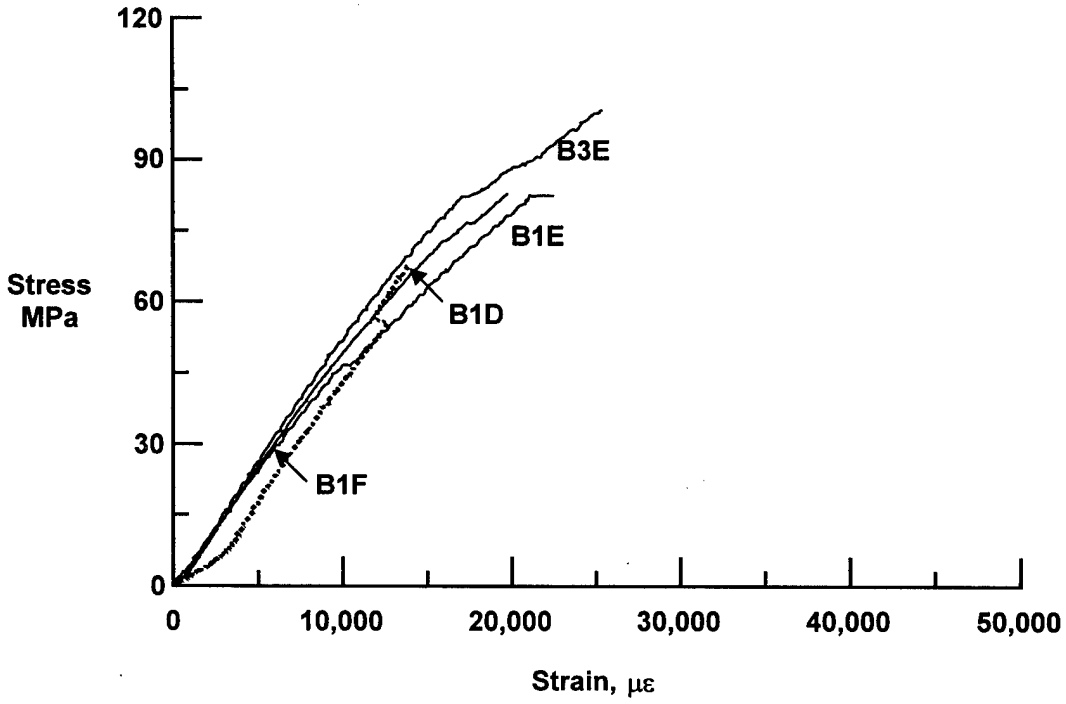

FIGURE 14. SHEAR STRESS-STRAIN RESPONSE OF BRAIDED COUPONS

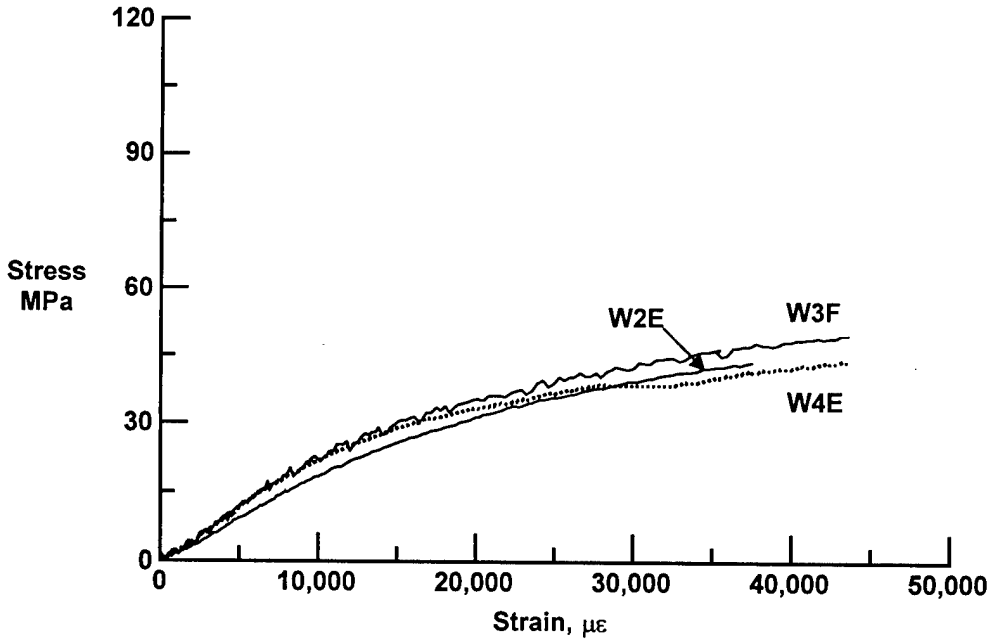

FIGURE 15. SHEAR STRESS-STRAIN RESPONSE OF WOVEN COUPONS

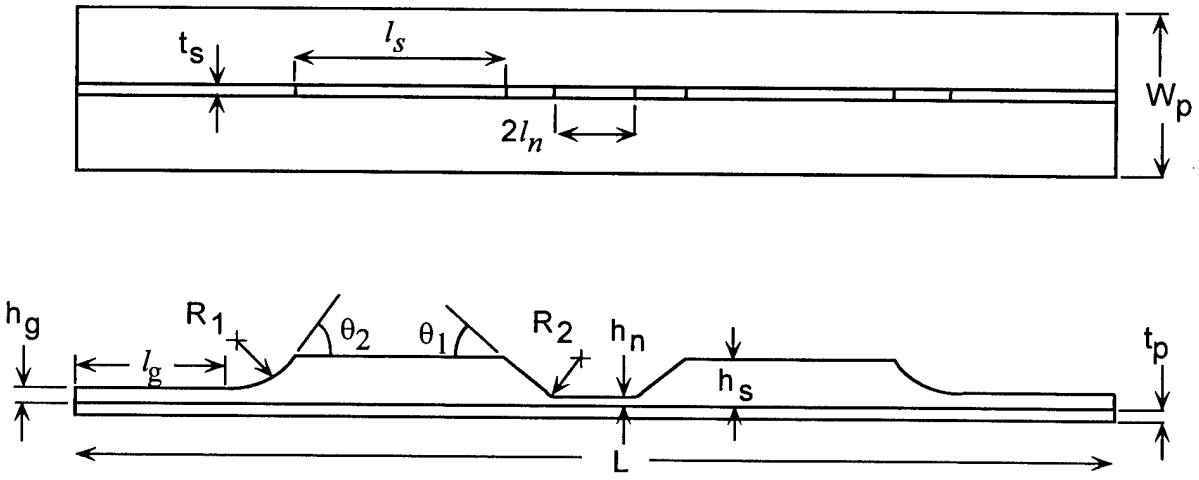

FIGURE 16. NC A&T INTEGRALLY BRAIDED AND WOVEN PANELS

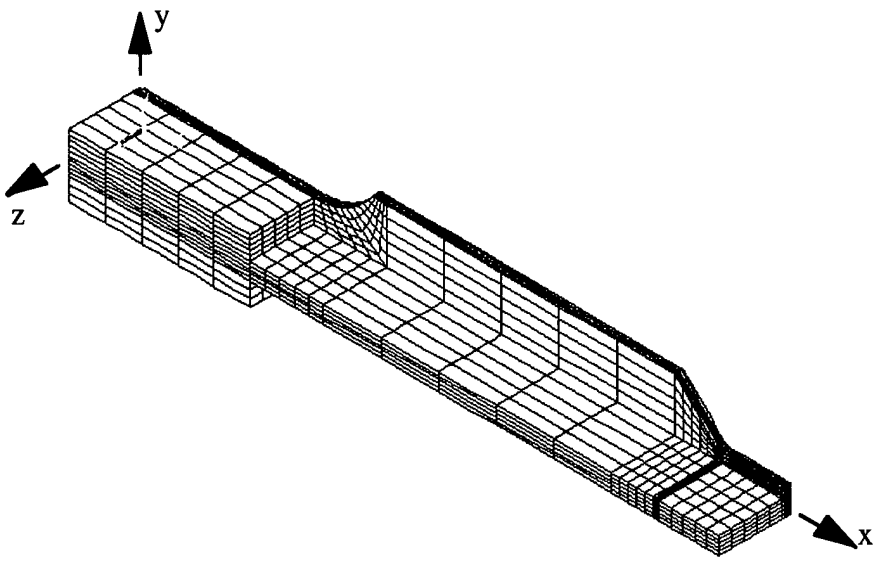

FIGURE 17. FINITE ELEMENT MODEL OF ONE-QUARTER OF THE SPECIMEN

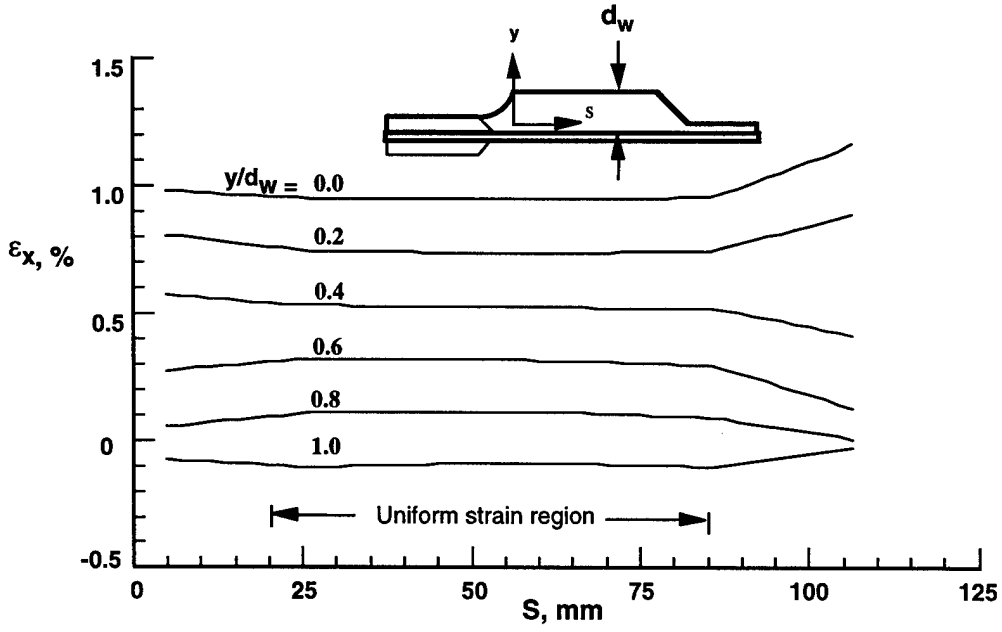

FIGURE 18. VARIATION OF ε_x ALONG THE STIFFENER AXIS AT VARIOUS DEPTHS (y/d_w) LOCATIONS ON z = 0 PLANE

FIGURE 19. DEFORMED SHAPE OF THE BRAIDED TEST PANEL
(Linear Analysis)

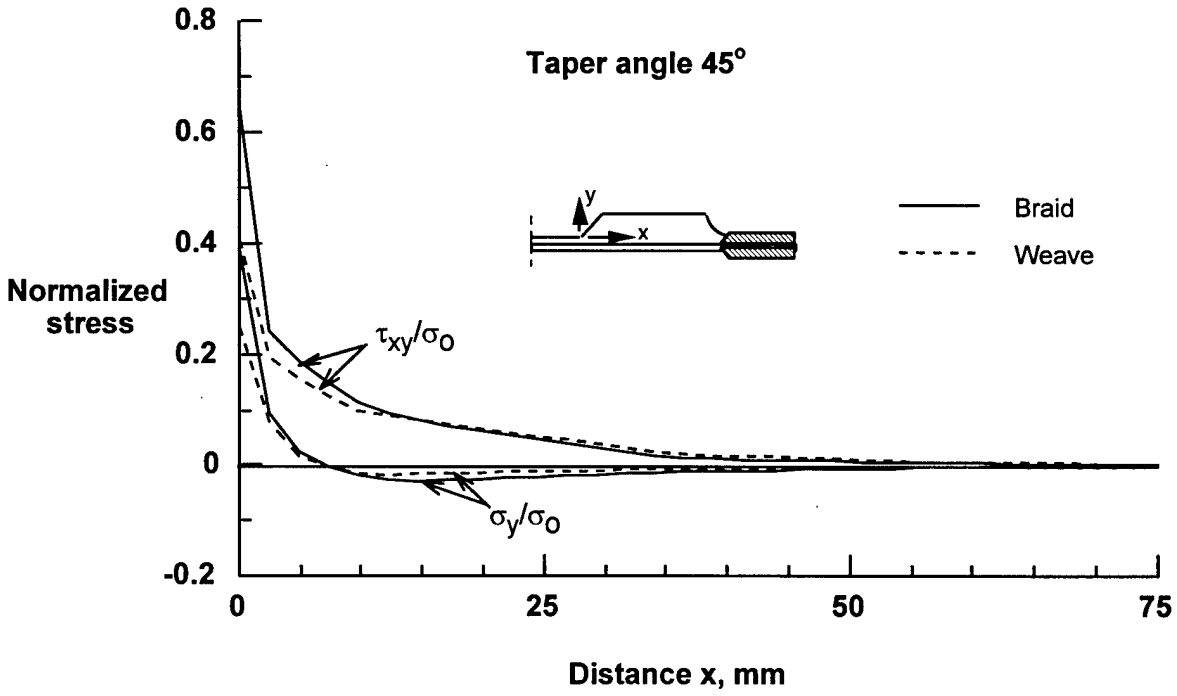

FIGURE 20. VARIATION OF NORMALIZED PEEL (σ_y) AND SHEAR (τ_{xy}) STRESS DISTRIBUTION FROM THE NOTCH ROOT INTO THE STIFFENER

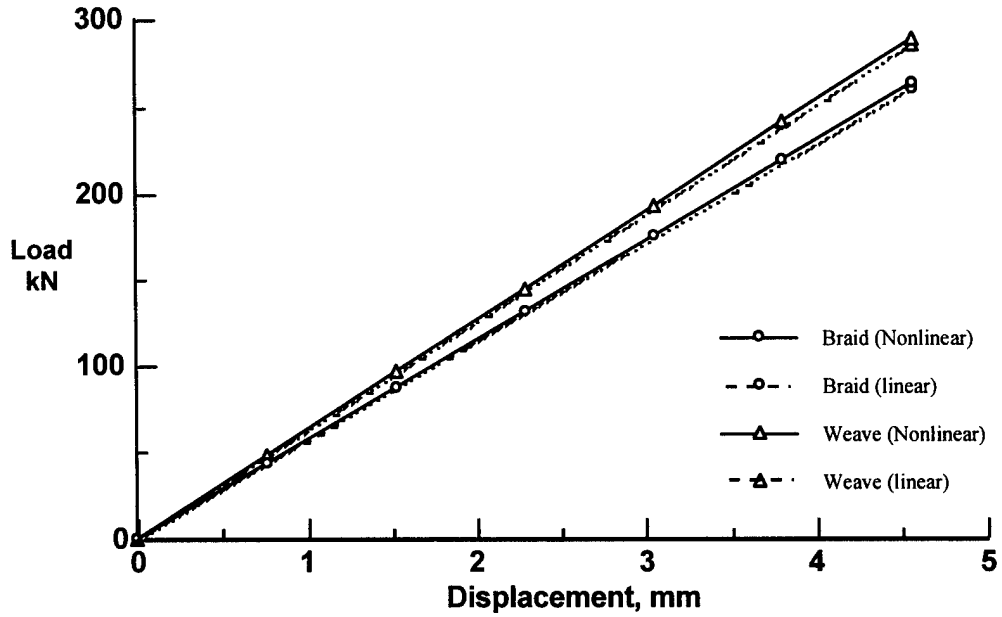

FIGURE 21. LOAD VERSUS DISPLACEMENT FROM LINEAR AND LARGE-DEFORMATION ANALYSES

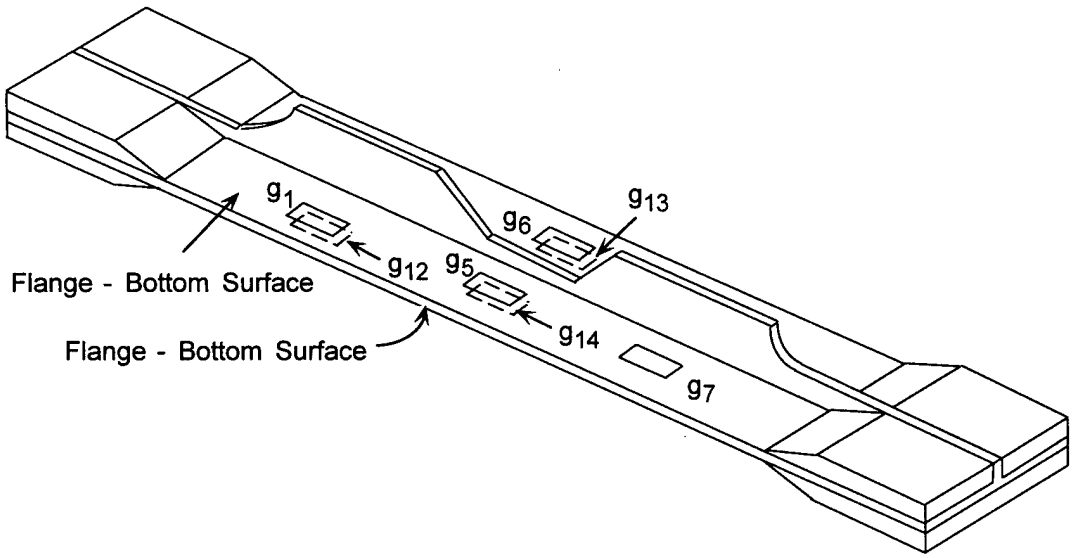

FIGURE 22. TEST SPECIMEN WITH STRAIN GAGES

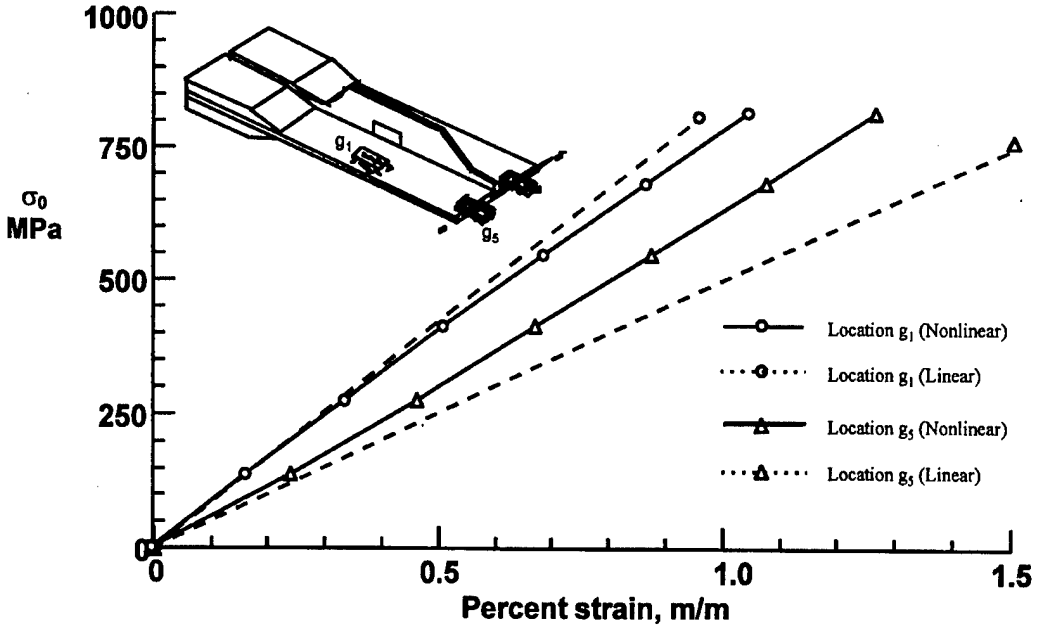

FIGURE 23. VARIATION OF AVERAGE STRESS (σ_0) WITH LOCAL STRAINS AT LOCATIONS g_1 AND g_5 FOR BRAIDED COMPOSITE PANEL

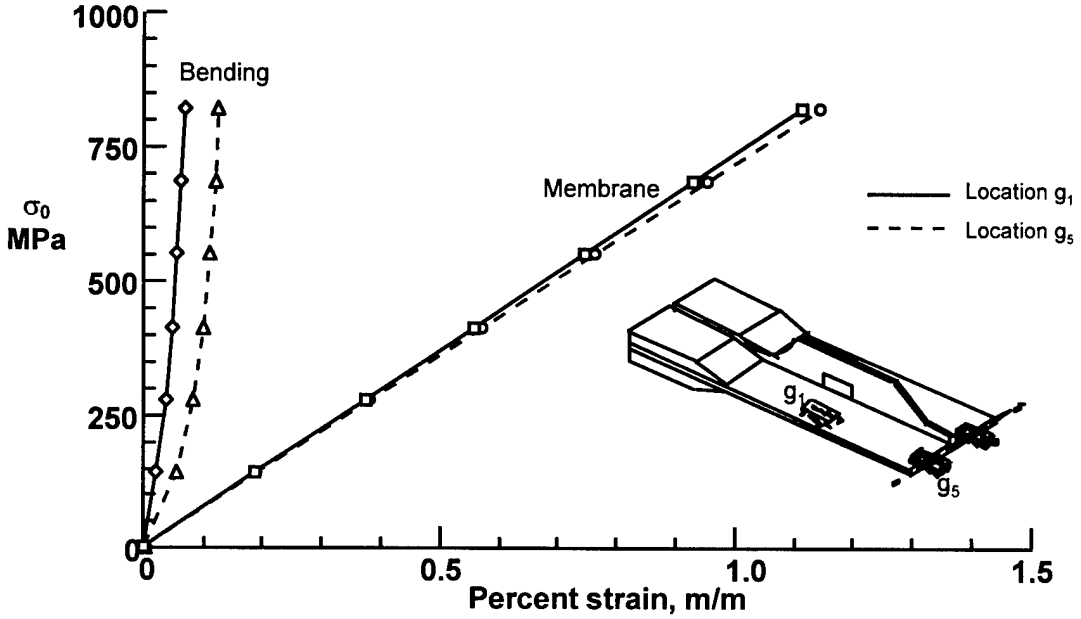

FIGURE 24. VARIATION OF MEMBRANE AND BENDING STRAIN WITH AVERAGE STRESS FOR BRAIDED COMPOSITE PANEL

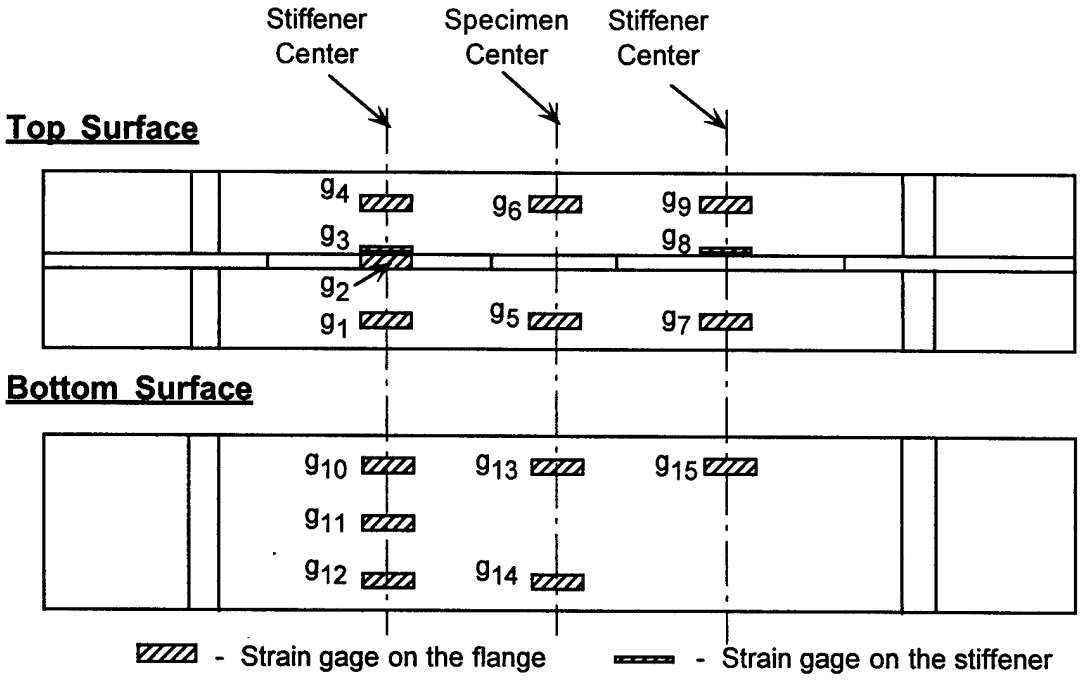

FIGURE 25. STRAIN GAGE LOCATIONS ON THE STIFFENED PANEL SPECIMEN

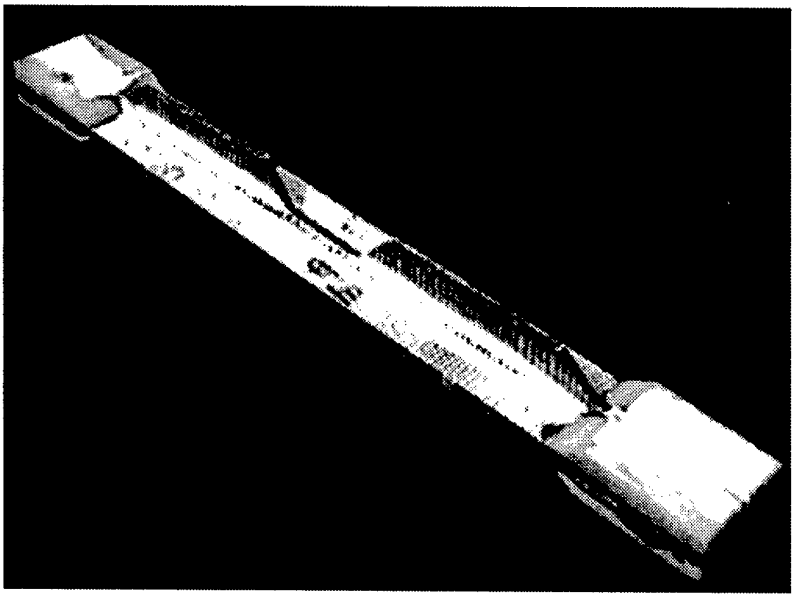

FIGURE 26. PHOTOGRAPH OF THE STIFFENED PANEL SPECIMEN

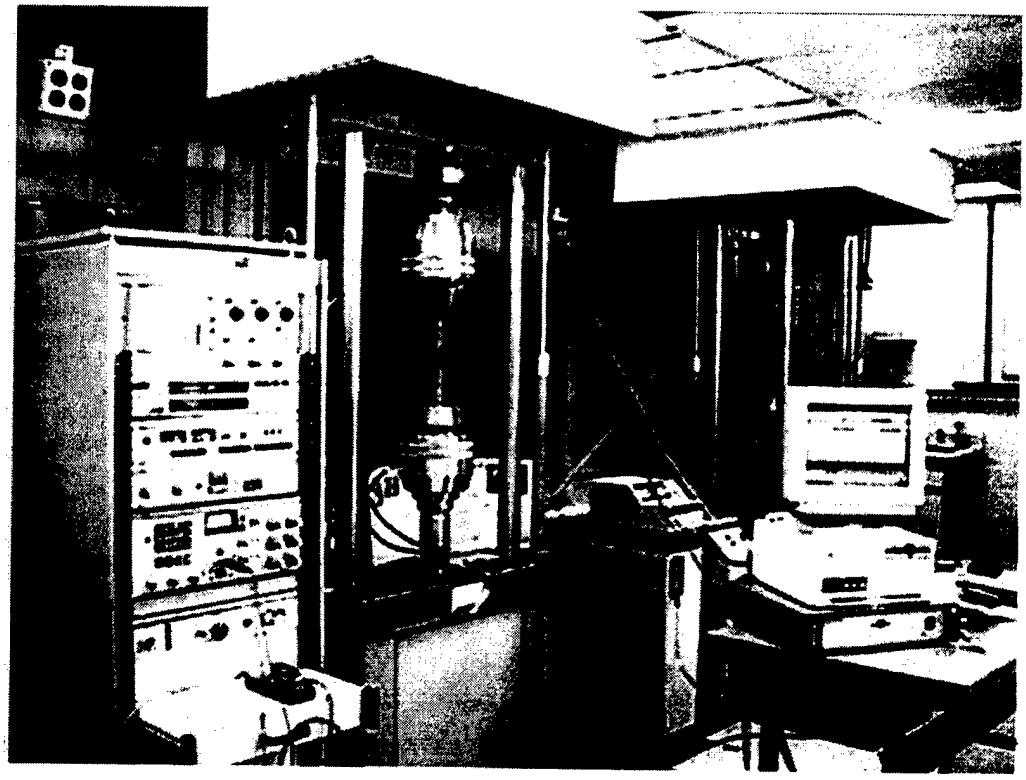

FIGURE 27. STIFFENED PANEL TEST EXPERIMENTAL SETUP

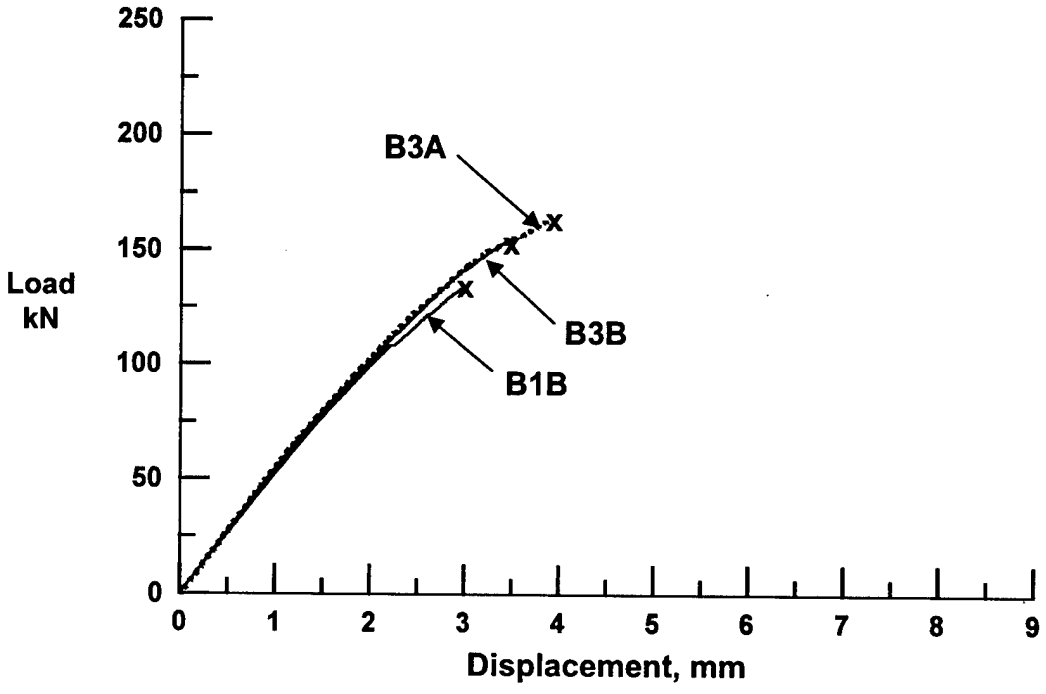

FIGURE 28. LOAD-DISPLACEMENT RESPONSE OF BRAIDED PANELS

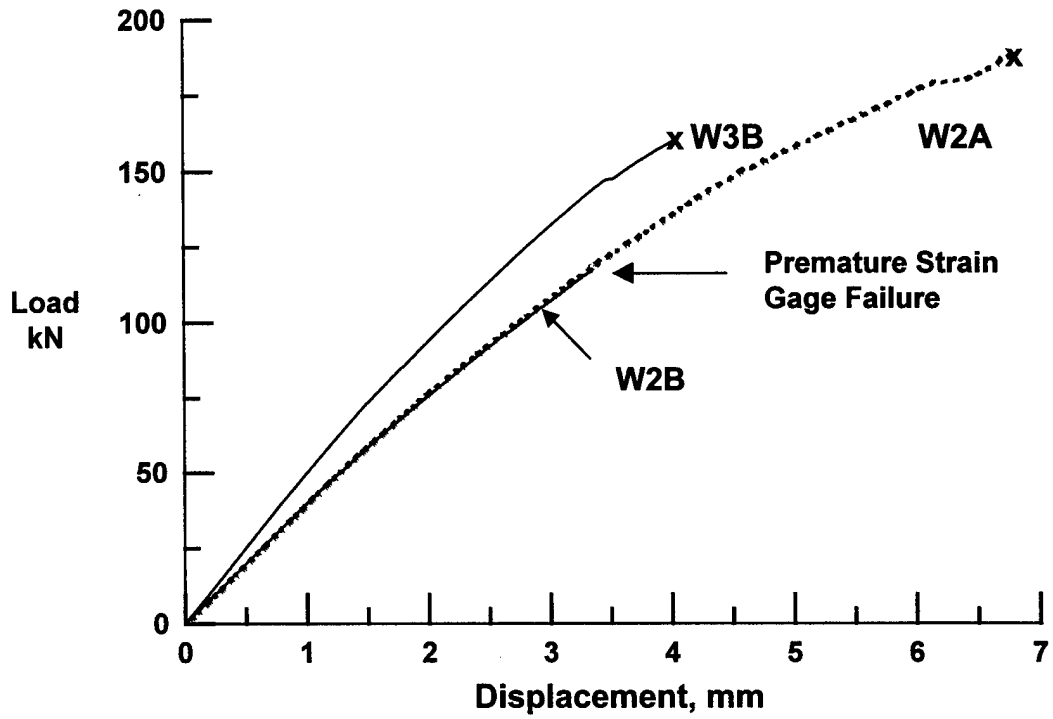

FIGURE 29. LOAD-DISPLACEMENT RESPONSE OF WOVEN COMPOSITE PANELS

FIGURE 30. FAILURE MODE OF A BRAIDED COMPOSITE PANEL

FIGURE 31. FAILURE MODE OF A WOVEN COMPOSITE PANEL

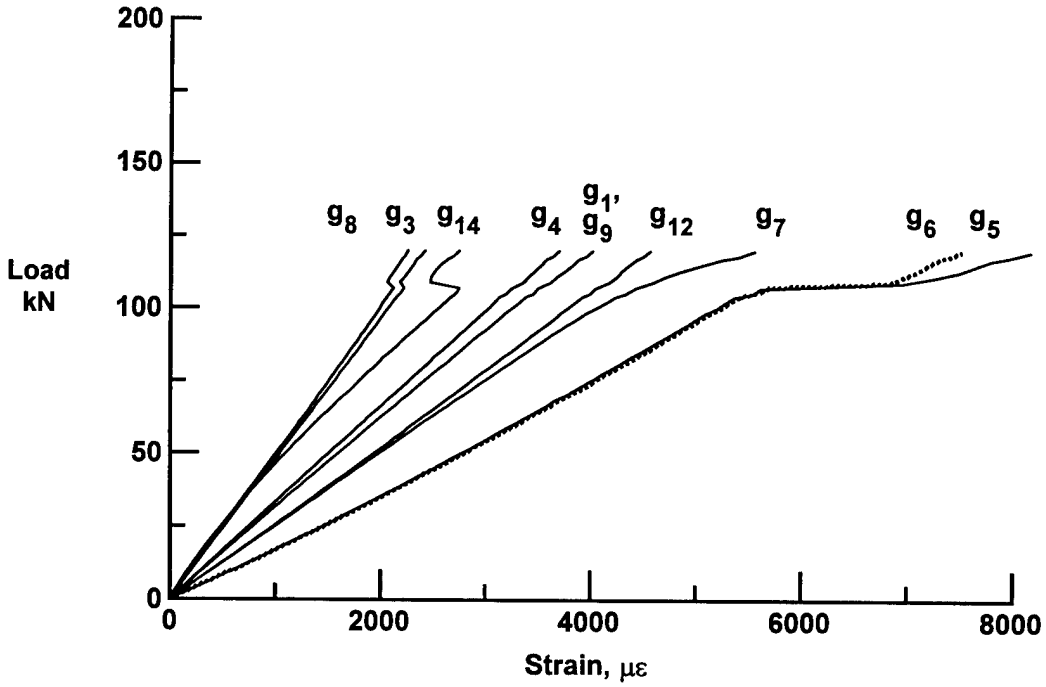

FIGURE 32. LOAD-STRAIN RESPONSE OF BRAIDED COMPOSITE PANEL B1B

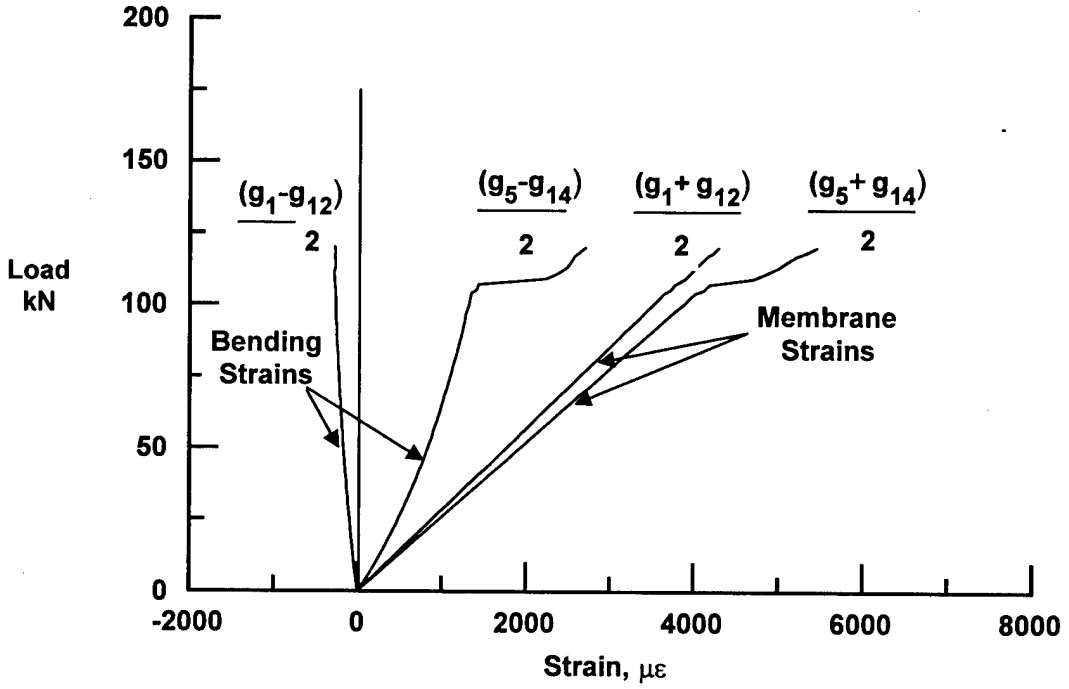

FIGURE 33. LOAD-STRAIN RESPONSE OF BRAIDED COMPOSITE PANEL B1B

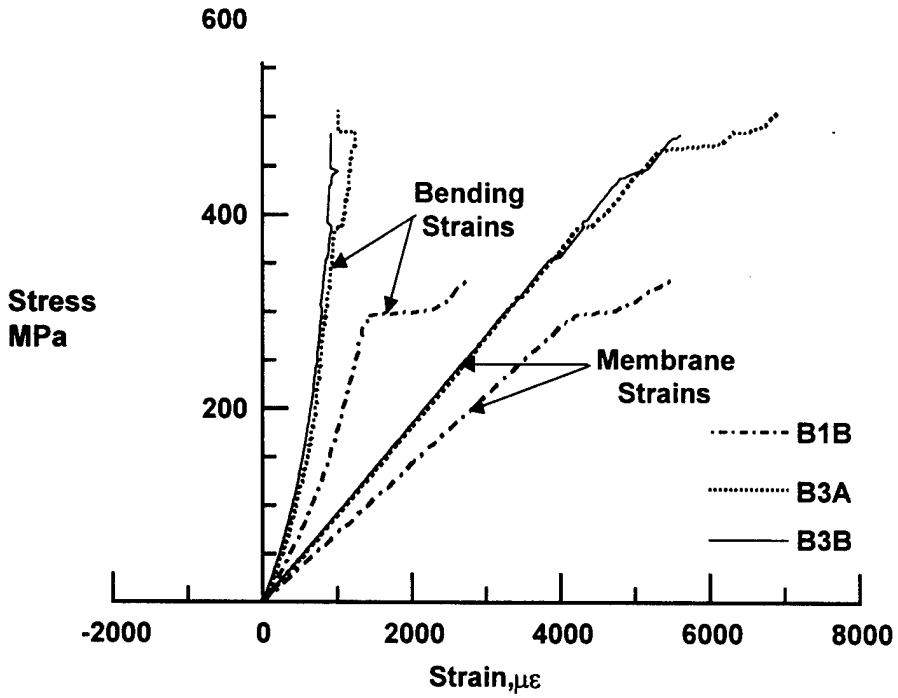

FIGURE 34. STRESS-STRAIN RESPONSE OF BRAIDED COMPOSITE PANELS AT THE NOTCH CENTER

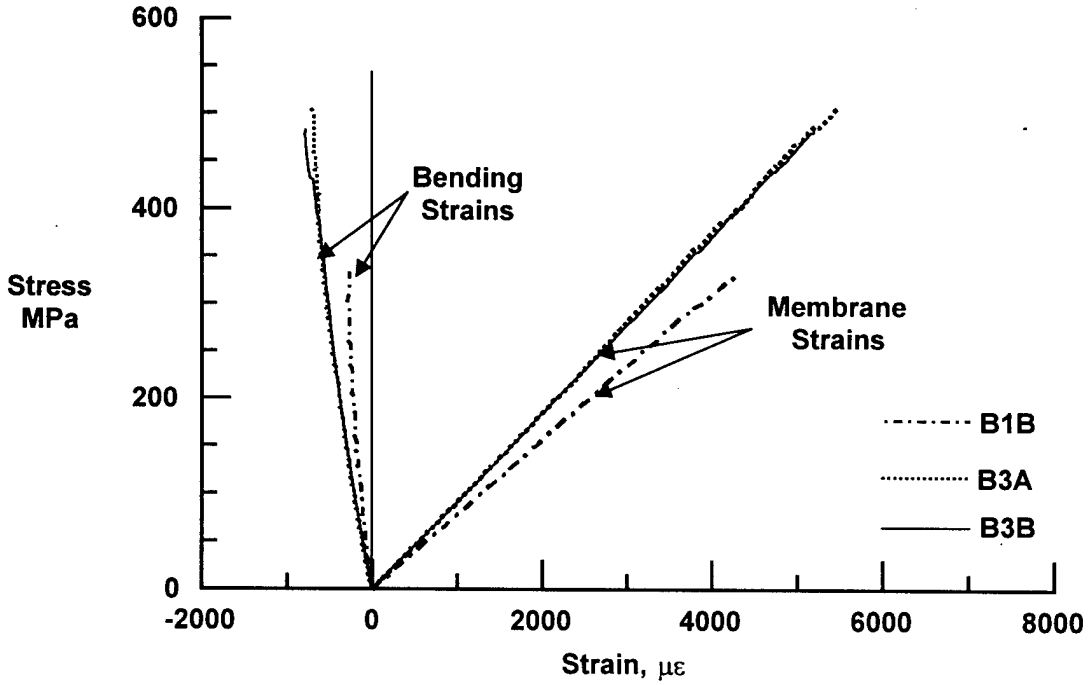

FIGURE 35. STRESS-STRAIN RESPONSE OF BRAIDED COMPOSITE PANELS AT THE CENTER OF THE STIFFENER

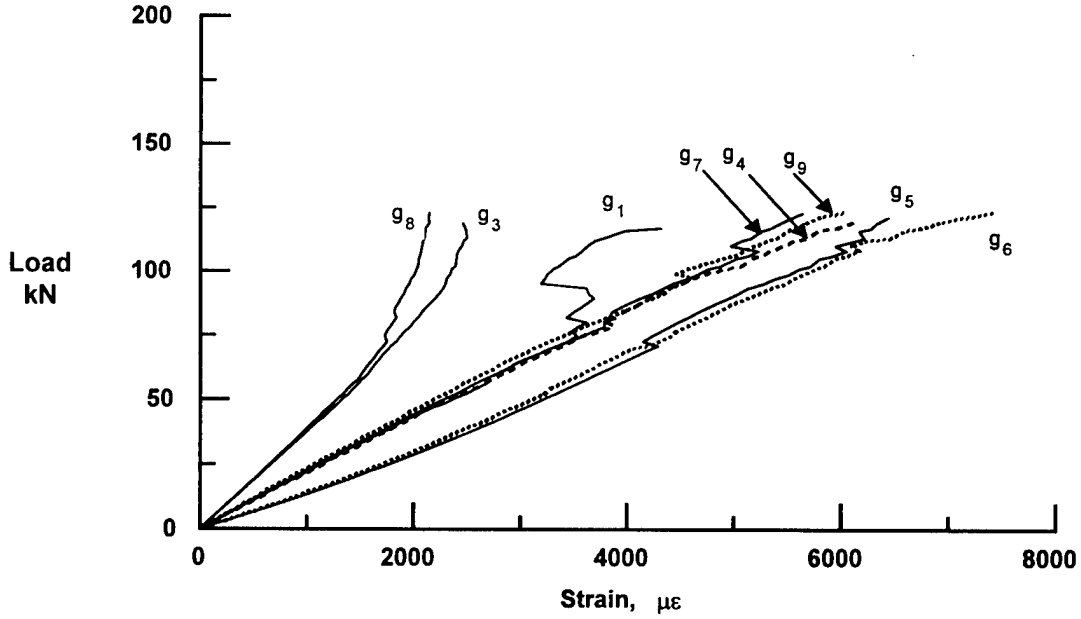

FIGURE 36. LOAD-STRAIN RESPONSE OF WOVEN COMPOSITE PANEL W2A

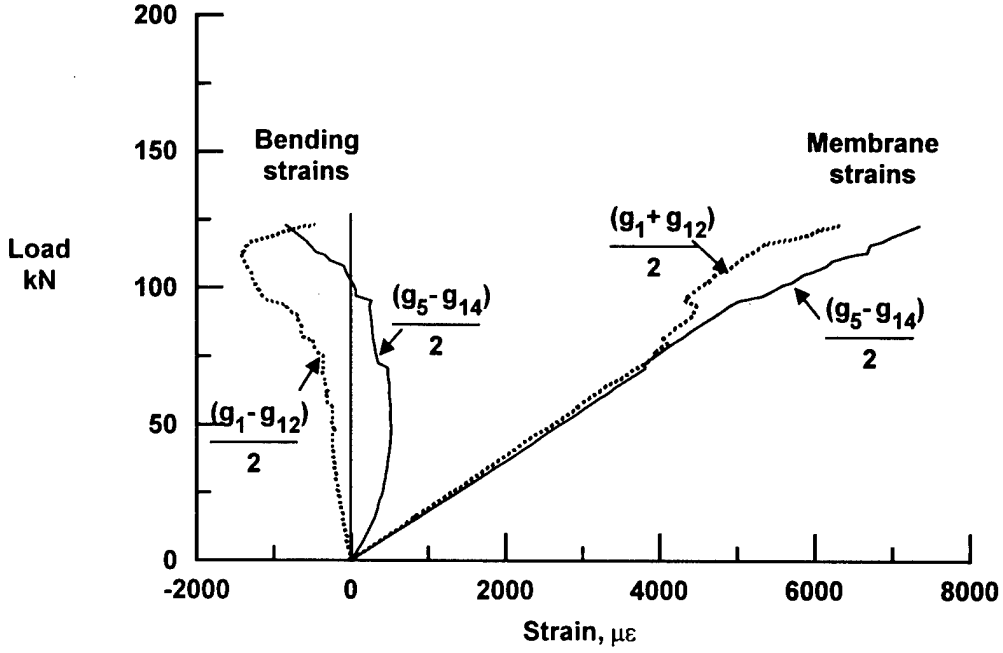

FIGURE 37. FLANGE MIDPLANE MEMBRANE AND BENDING STRAINS

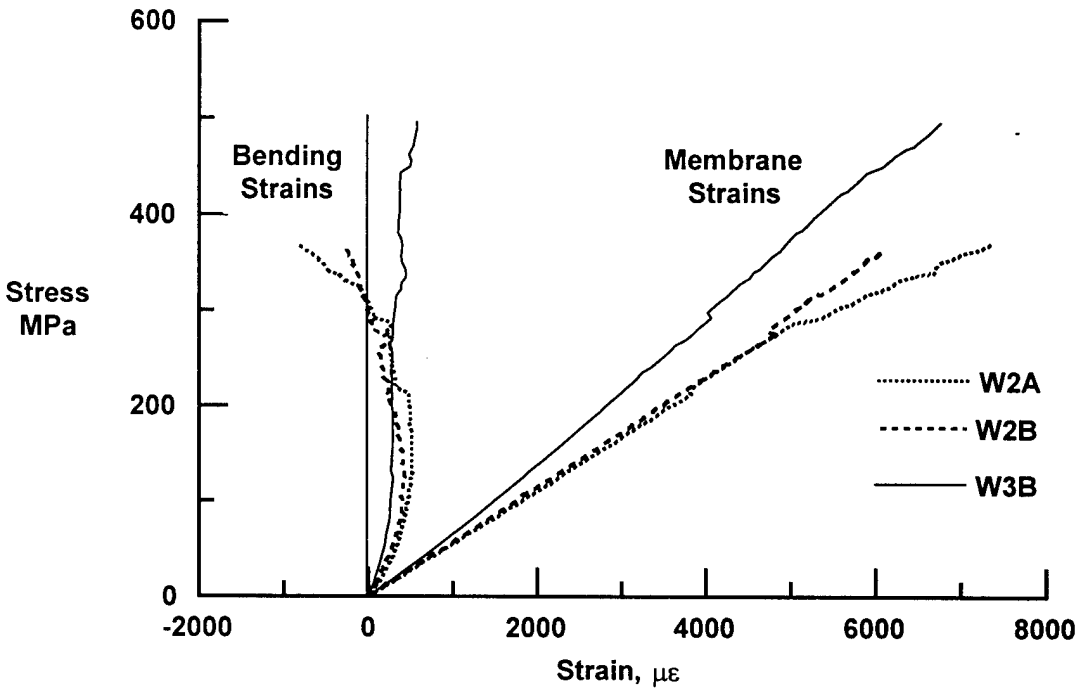

FIGURE 38. STRESS-STRAIN RESPONSE OF WOVEN COMPOSITE PANELS AT THE CENTER OF THE NOTCH

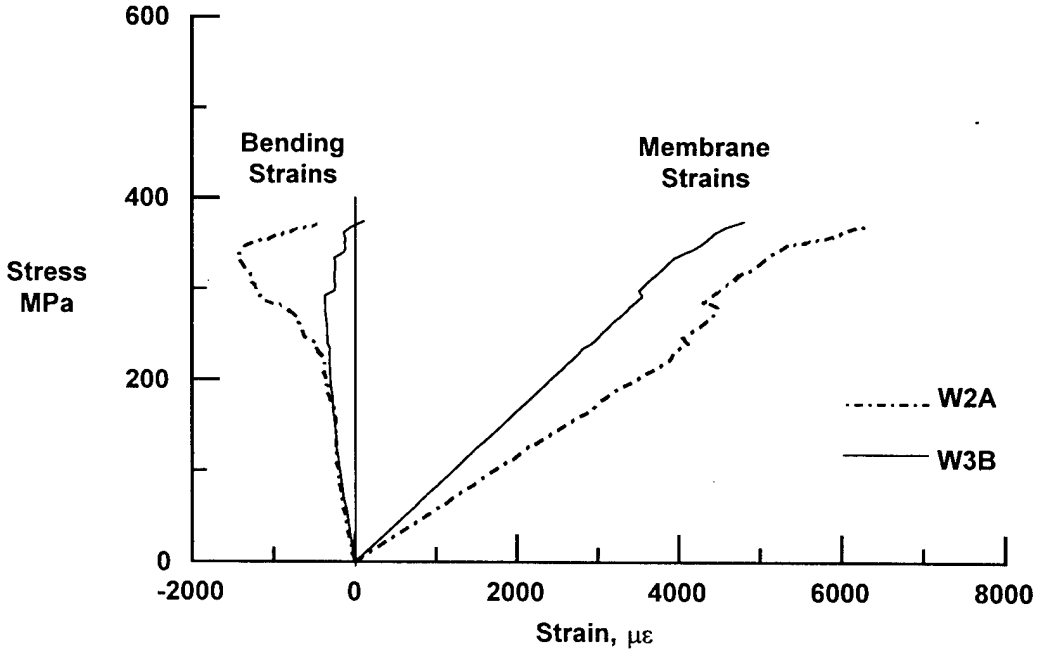

FIGURE 39. STRESS-STRAIN RESPONSE OF WOVEN COMPOSITE PANELS AT THE CENTER OF THE STIFFENER

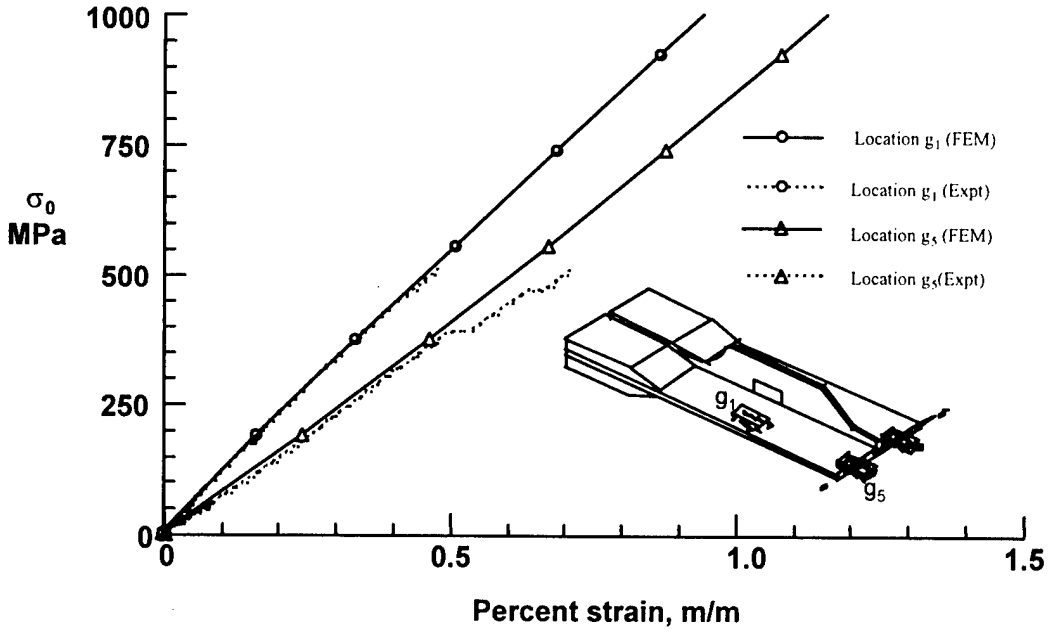

FIGURE 40. COMPARISON OF TEST AND ANALYSIS OF LOCAL STRAIN VARIATION FOR BRAIDED COMPOSITE PANEL B3A

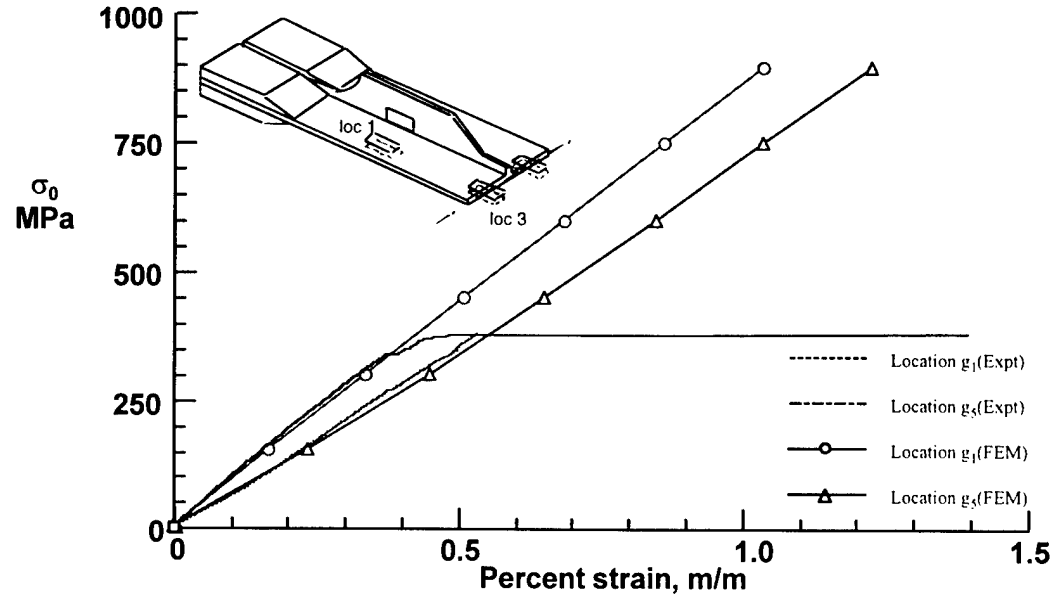

FIGURE 41. COMPARISON OF TEST AND ANALYSIS OF LOCAL STRAIN VARIATION FOR WOVEN COMPOSITE PANEL W2A

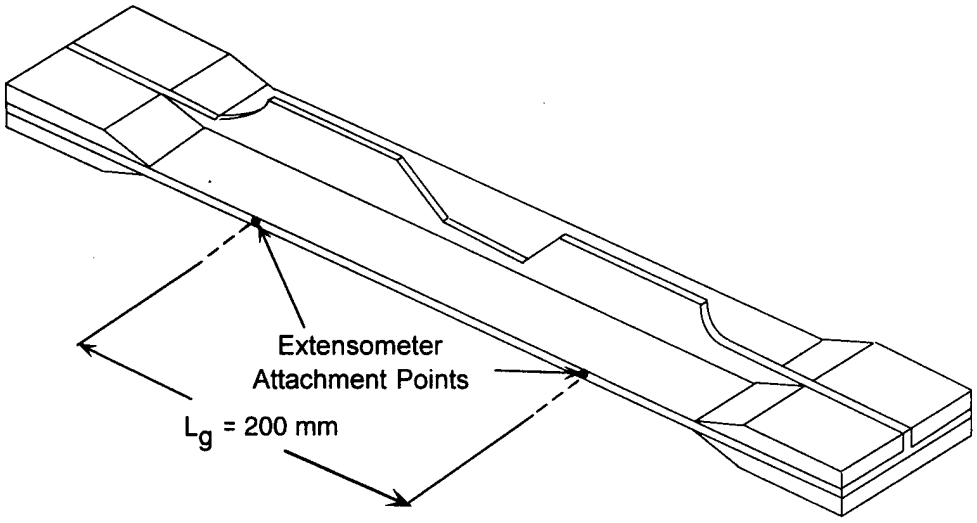

FIGURE 42. FATIGUE TEST SPECIMEN AND EXTENSOMETER ATTACHMENT POINTS

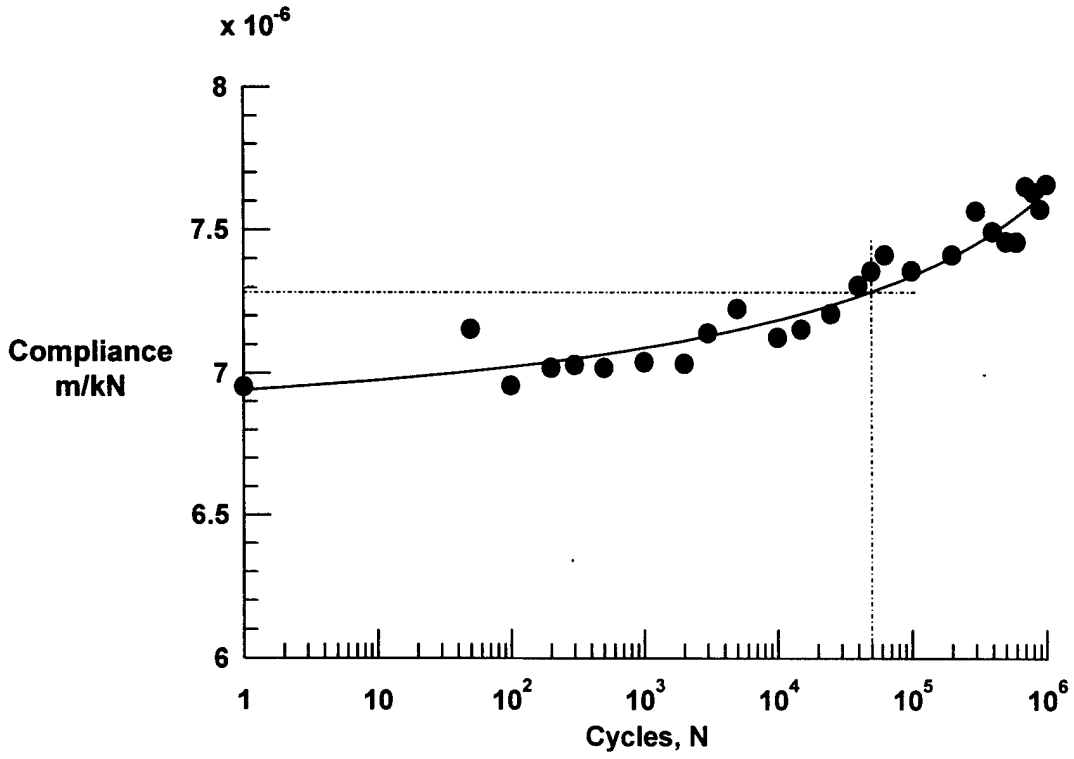

FIGURE 43. VARIATION OF THE COMPLIANCE AS A FUNCTION OF FATIGUE CYCLES FOR THE BRAIDED COMPOSITE PANEL B1A

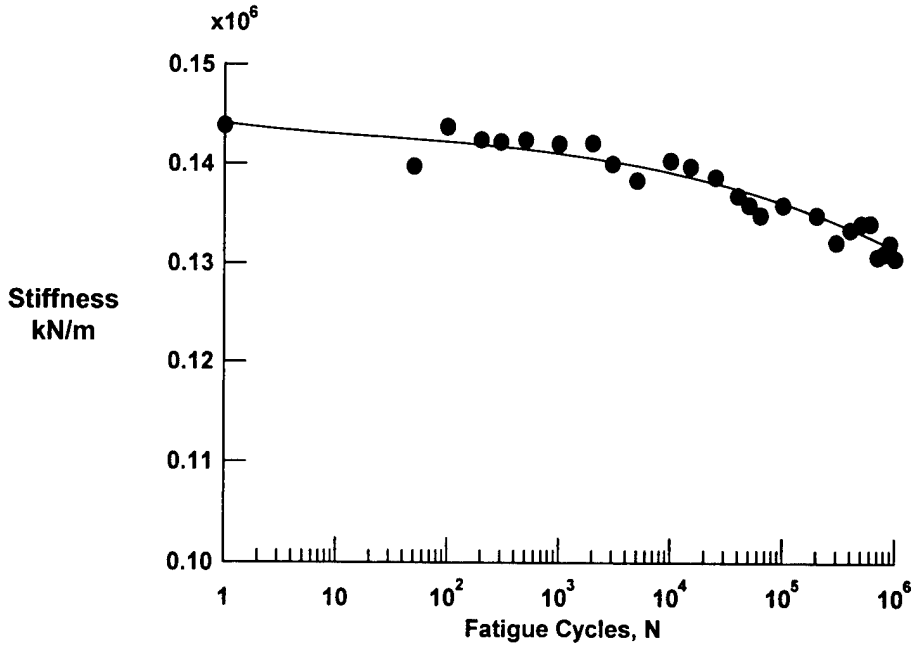

FIGURE 44. VARIATION OF THE STIFFNESS AS A FUNCTION OF FATIGUE CYCLES FOR THE BRAIDED COMPOSITE PANEL B1A

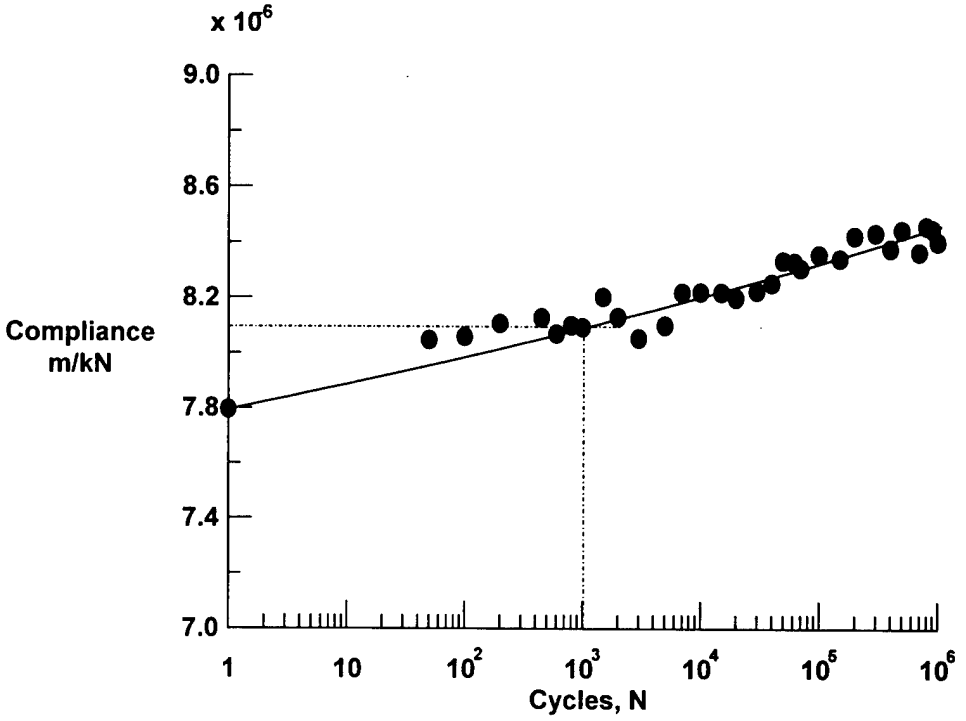

FIGURE 45. VARIATION OF THE COMPLIANCE AS A FUNCTION OF FATIGUE CYCLES FOR THE WOVEN COMPOSITE PANEL W3A

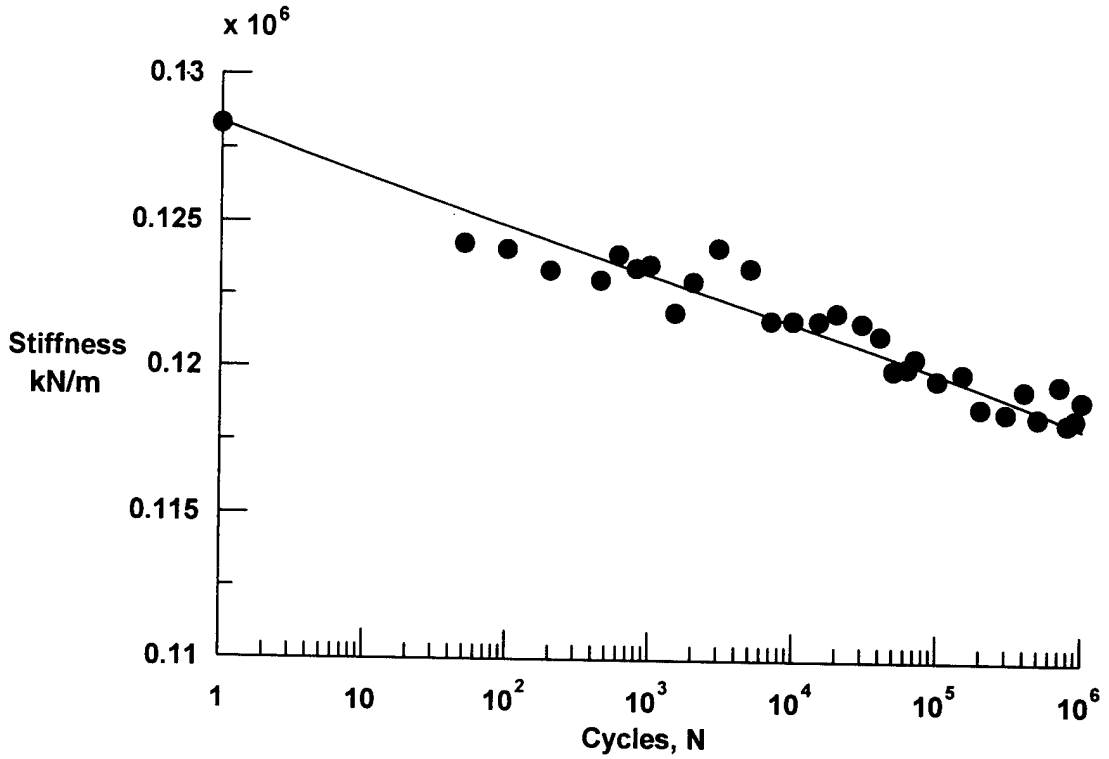

FIGURE 46. VARIATION OF THE STIFFNESS AS A FUNCTION OF FATIGUE CYCLES FOR THE WOVEN COMPOSITE PANEL W3A

TABLE 1. TENSILE PROPERTIES OF BRAIDED AND WOVEN COMPOSITES

Specimen No.	Length (mm)	Width (mm)	Thickness (mm)	E_x (GPa)	V_{xy}	Strength (MPa)
Braided Coupons						
B1C	152.4	26.9	6.4	52.72	0.96	351.2
B3C	152.4	26.1	5.8	54.03	0.90	347.4
B3D	152.4	26.4	5.8	67.15	0.77	451.7
Average Properties				57.97	0.88	383.4
Standard Deviation				7.98	0.10	59.2
Woven Coupons						
W2C	152.4	25.0	6.0	52.68	0.05	N.F.
W2D	152.4	25.9	6.0	52.01	0.06	N.F.
W3C	152.4	25.5	5.9	73.52	0.06	N.F.
W4C*	152.4	25.6	6.0	NA	NA	708.0**
W4D*	152.4	22.9	6.0	NA	NA	641.0**
Average Properties				59.40	0.05	64.5**
Standard Deviation				12.23	0.003	47.4**

N.F. No failure of the specimen, tabs debonded

* Not instrumented with strain gages; E_x and ν not measured

** Specimens failed in the grip region

TABLE 2. SHEAR PROPERTIES OF BRAIDED AND WOVEN PANELS

Specimen No.	Thickness (mm)	G_{xy} (GPa)	Shear Yield Strength (MPa)
Braided Specimens			
B1D	6.40	5.51	69.5
B1E	6.40	4.96	52.5
B1F	6.40	5.59	N.A.
B3E	5.84	5.52	82.0
Average G_{xy}		5.39	68.0
Standard Deviation		0.29	14.8
Woven Specimens			
W2E	5.99	2.19	24.7
W3F	5.87	2.78	26.8
W4E	6.02	2.57	25.3
Average G_{xy}		2.51	25.6
Standard Deviation		0.30	1.1

TABLE 3. IN SITU PROPERTIES USED IN THE ANALYSIS

Property	Braided Panel (B3A) GPa (Msi)	Woven Panel (W3B) GPa (Msi)
E_x	67.2 (9.74)	73.5 (10.66)
E_y^*	7.9 (1.15)	44.1 (6.40)
E_z^*	7.6 (1.11)	44.1 (6.40)
G_{xy}	5.5 (0.80)	2.8 (0.41)
G_{yz}^*	2.8 (0.41)	2.8 (0.41)
G_{xz}^*	3.3 (0.48)	2.8 (0.41)
ν_{xy}	0.77	0.06
ν_{yz}^*	0.33	0.06
ν_{xz}^*	0.15	0.06

* Estimated using TEXCAD3D [4]

TABLE 4. STRESS AND STRAIN CONCENTRATION FACTORS

Taper Angle	Stress Concentration Factors			Strain Concentration Factor
	K_x	K_y	K_{xy}	K_{ex}
3D Braids				
45	4.10	0.39	0.80	4.77
60	3.77	0.40	0.75	4.45
75	3.83	0.42	0.82	4.55
3D Weaves				
45	3.87	0.27	0.50	4.56
60	3.92	0.40	0.34	4.62
75	3.96	0.40	0.51	4.68

TABLE 5. SUMMARY OF RESULTS FROM PANEL SPECIMEN TESTS

Specimen No.	Cross-Sectional Area at Notch (mm^2)	Cross-Sectional Area at Stiffener Center (mm^2)	Failure Load (kN)	Fracture Strength (MPa)	Axial Modulus (GPa)
Braided Composite Panels					
B1B	362.1	460.5	133.4	368.5	71.20
B3A	322.2	414.7	163.7	508.1	91.42
B3B	319.3	409.6	154.8	484.8	92.27
BT0	359.7	466.5	133.4	370.8	71.00
BT1	411.5	515.1	179.6	436.5	75.90
Average Properties				433.7	80.36
Standard Deviation				63.9	10.67
Woven Composite Panels					
W2A*	333.4	427.3	179.3	565.7 (600.0†)	54.37
W2B	328.8	430.3	204.8	622.9 (661.4†)	59.44
W3B	320.5	411.0	160.1	499.6 (530.3†)	74.29
WT0	341.8 (425.8**)	430.9 (511.8)	198.7	581.4 (613.9†)	87.60
WT1*	343.3 (429.9**)	431.0 (517.3)	219.5	639.4 (674.5†)	82.80
Average Properties				581.8 (616.0†)	71.70
Standard Deviation				54.8 (57.2†)	14.43

* Tab debonded

** Areas of the woven panels before the width was reduced

† Strength based on the flange areas only

APPENDIX A—LOAD-STRAIN PLOTS

The measurement of strain as a function of applied load for the braided specimens B3A, B3B, BT0, and BT1 and woven specimens W2B, W3B, WT0, and WT1 are provided in this appendix. The plots include the strains at the different strain gage locations and the bending and membrane strain components at the center of the stiffener segment and the center of the notched section. In many cases strain was not measured to specimen failure because of strain gage failure.

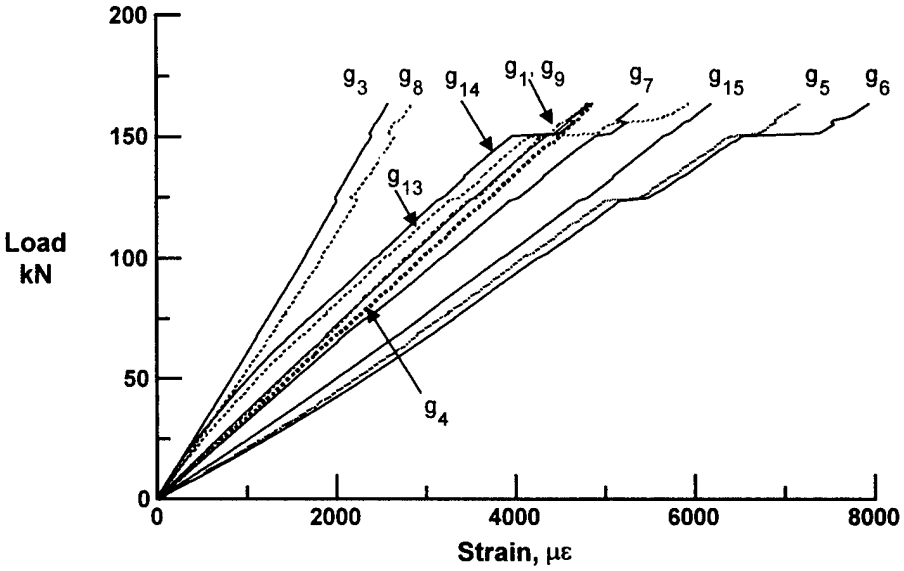

FIGURE A-1. LOAD-STSRAIN RESPONSE OF BRAIDED COMPOSITE PANEL B3A

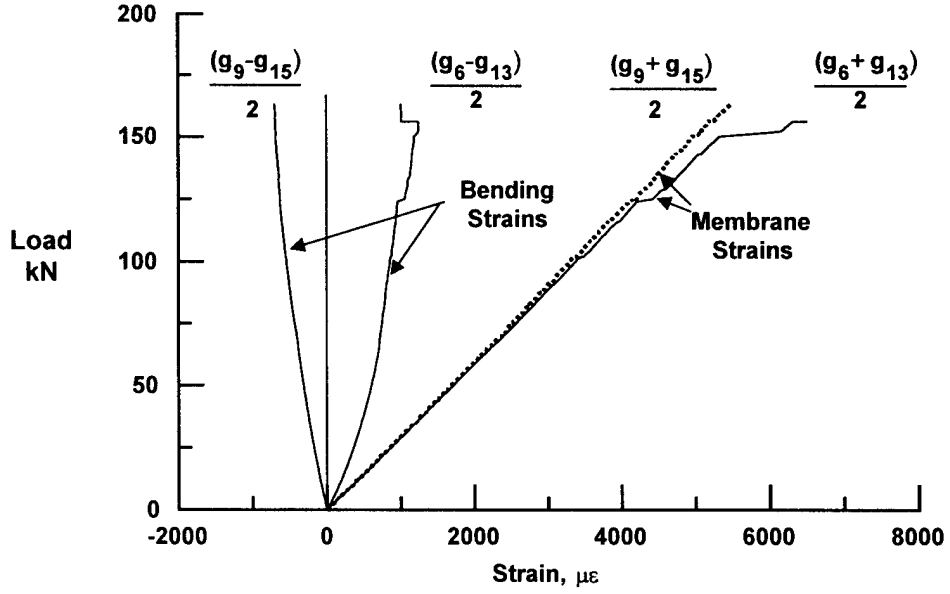

FIGURE A-2. MEMBRANE AND BENDING STRAINS OF BRAIDED COMPOSITE PANEL B3A

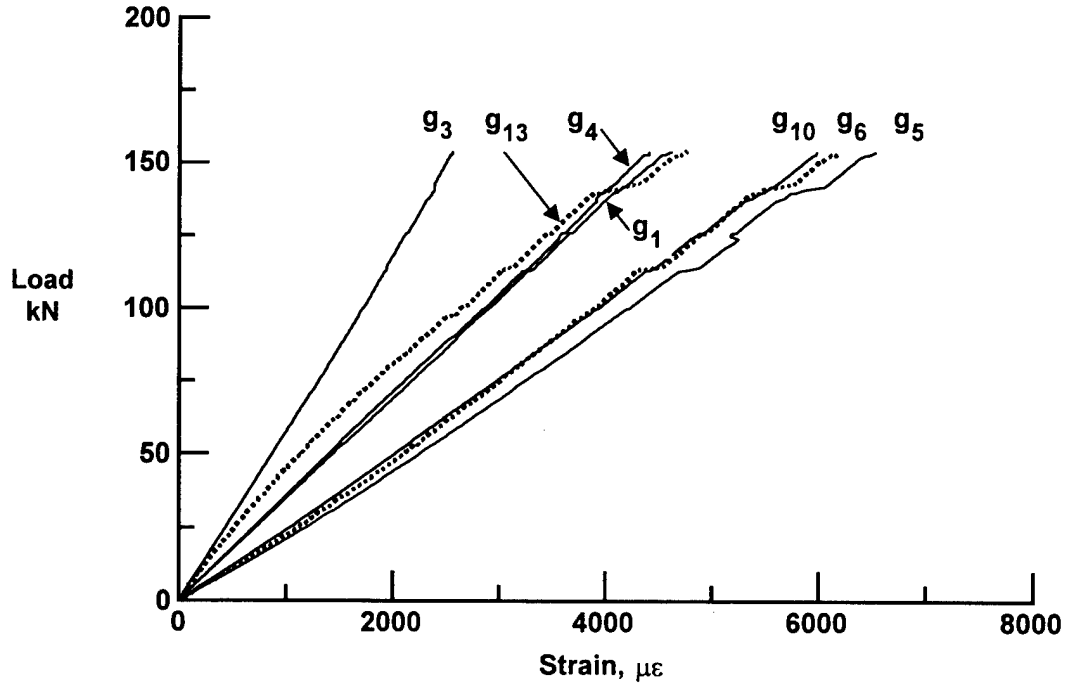

FIGURE A-3. LOAD-STRAIN RESPONSE OF BRAIDED COMPOSITE PANEL B3B

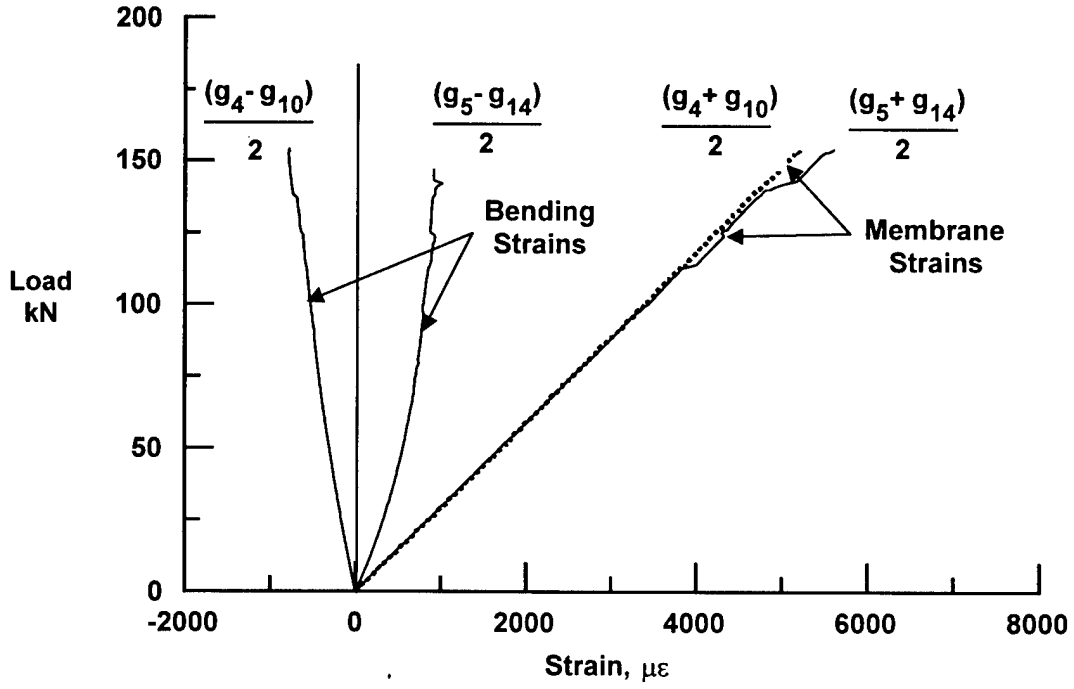

FIGURE A-4. MEMBRANE AND BENDING STRAINS OF BRAIDED COMPOSITE PANEL B3B

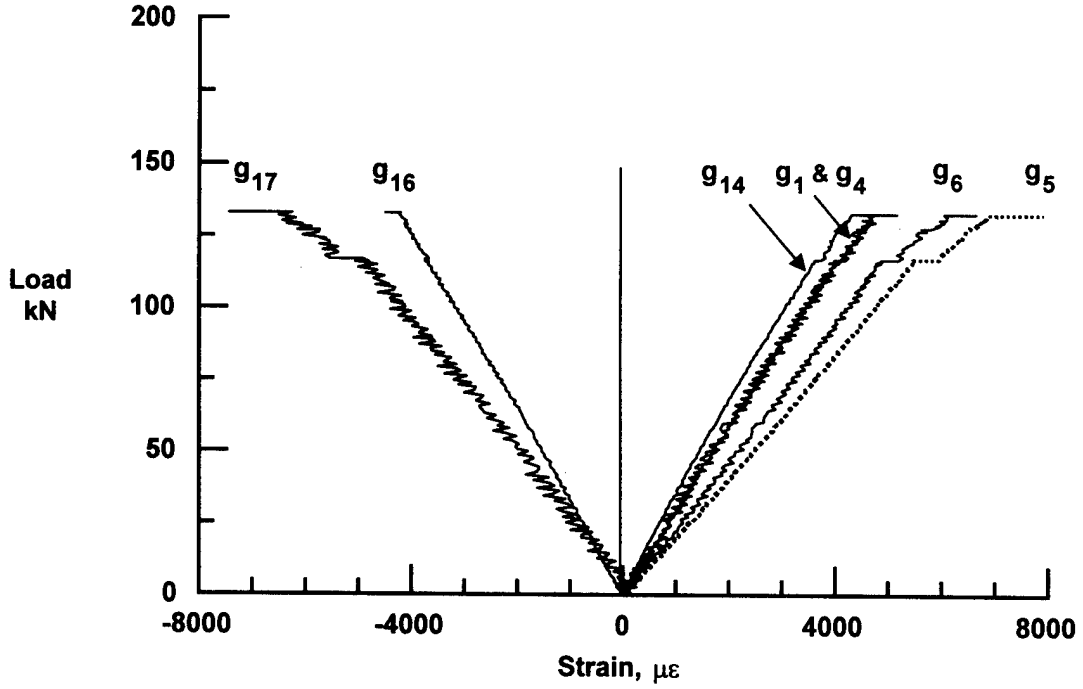

FIGURE A-5. LOAD-STRAIN RESPONSE OF BRAIDED COMPOSITE PANEL BT0

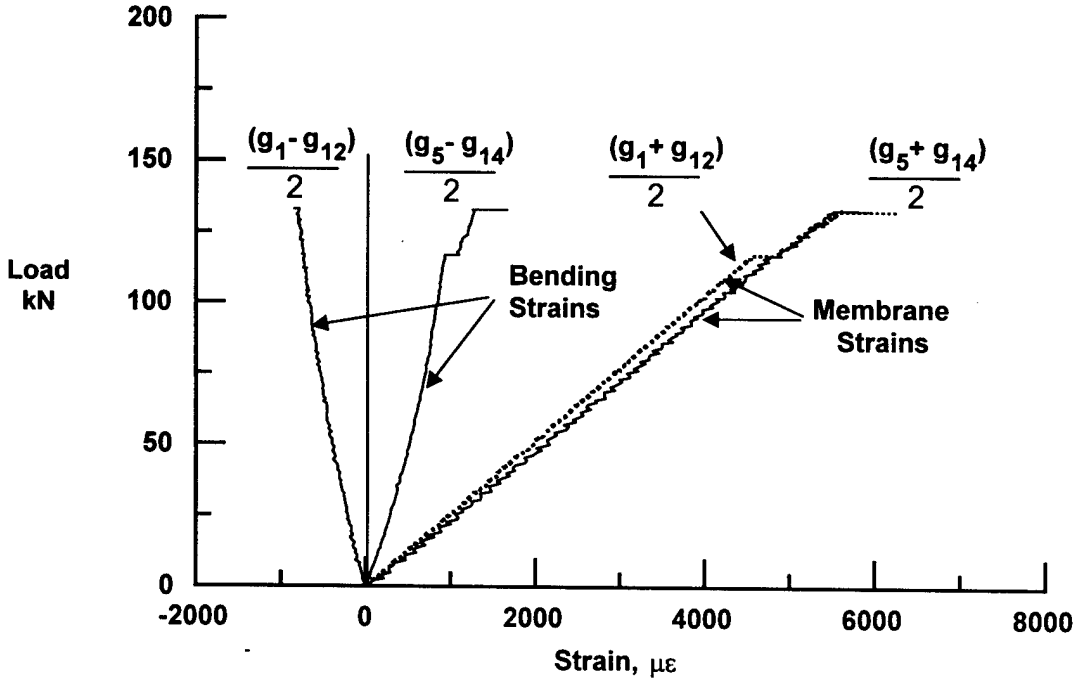

FIGURE A-6. MEMBRANE AND BENDING STRAINS OF BRAIDED COMPOSITE PANEL BT0

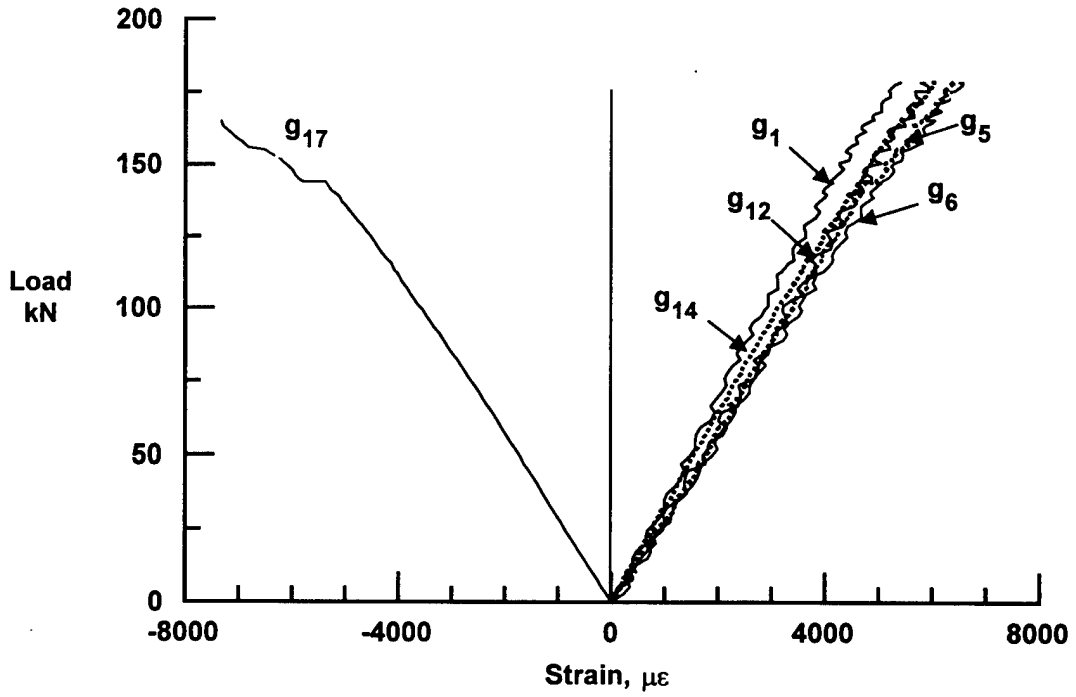

FIGURE A-7. LOAD-STRAIN RESPONSE OF BRAIDED COMPOSITE PANEL BT1

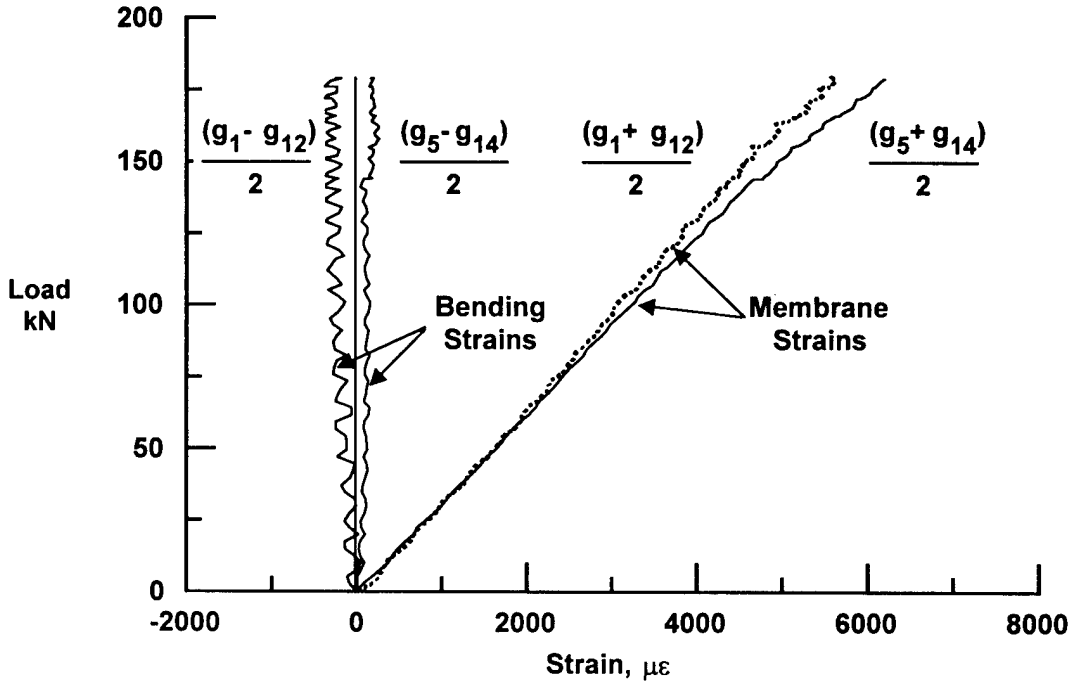

FIGURE A-8. MEMBRANE AND BENDING STRAINS OF BRAIDED COMPOSITE PANEL BT1

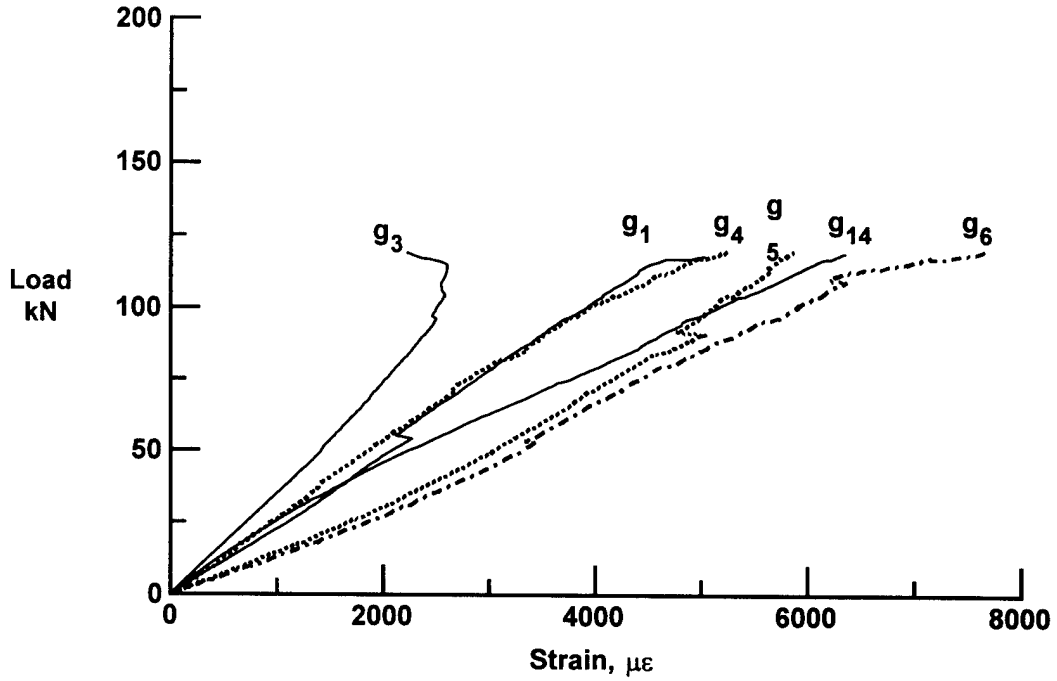

FIGURE A-9. LOAD-STRAIN RESPONSE OF WOVEN COMPOSITE PANEL W2B

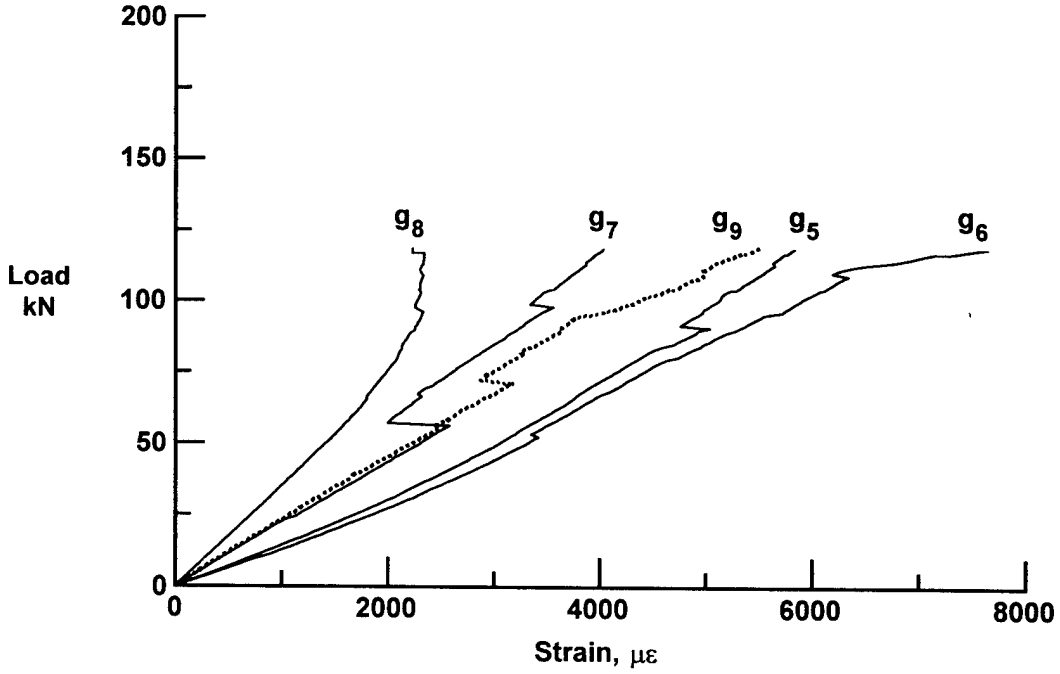

FIGURE A-10. LOAD-STRAIN RESPONSE OF WOVEN COMPOSITE PANEL W2B

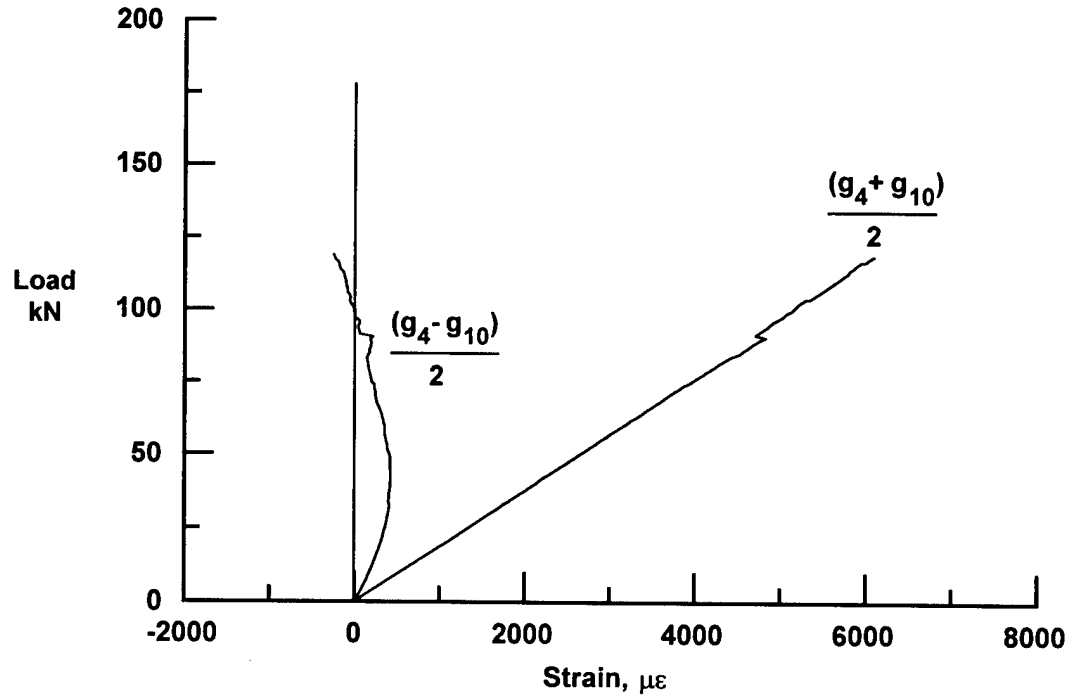

FIGURE A-11. MEMBRANE AND BENDING STRAINS OF WOVEN COMPOSITE PANEL W2B

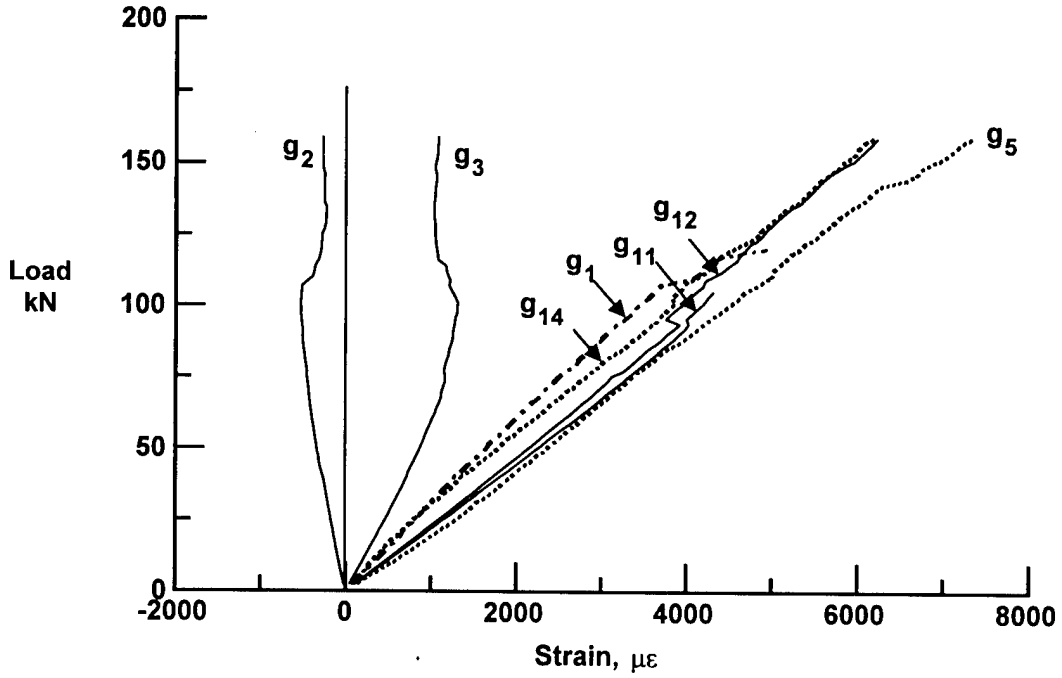

FIGURE A-12. LOAD-STRAIN RESPONSE OF WOVEN COMPOSITE PANEL W3B

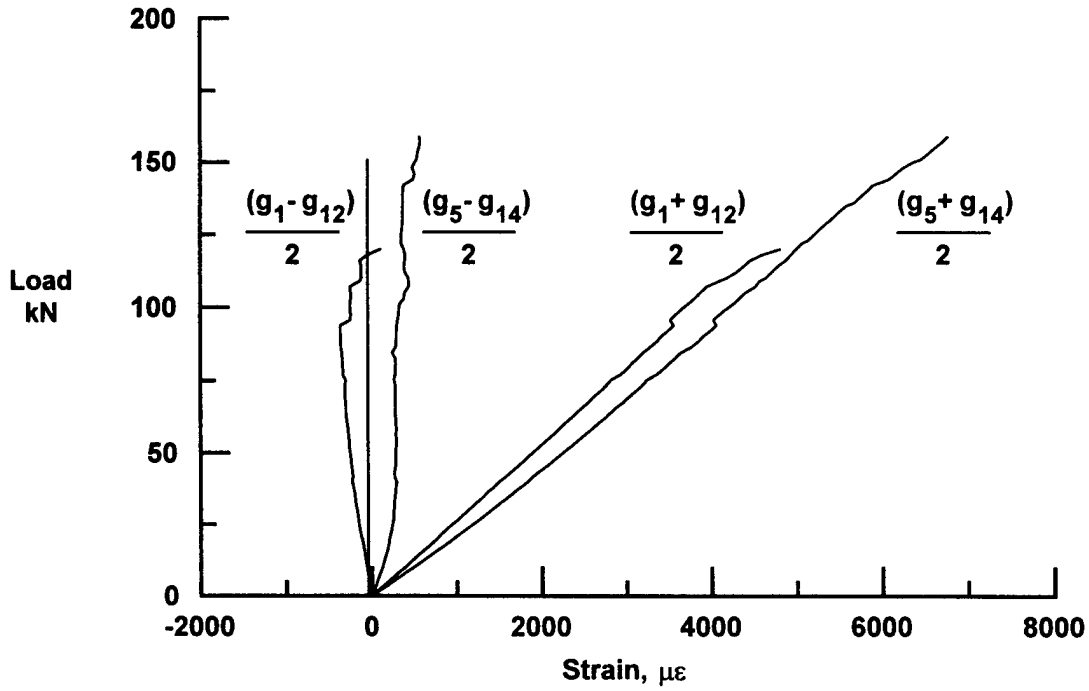

FIGURE A-13. MEMBRANE AND BENDING STRAINS OF WOVEN COMPOSITE PANEL W3B

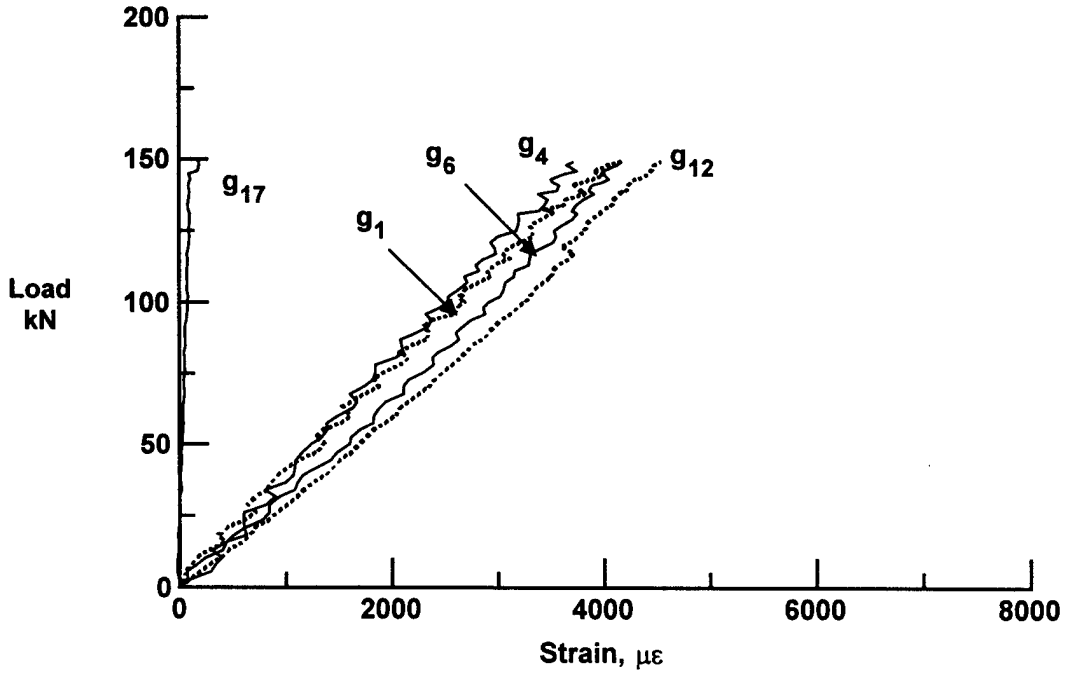

FIGURE A-14. LOAD-STRAIN RESPONSE OF WOVEN COMPOSITE PANEL WT0

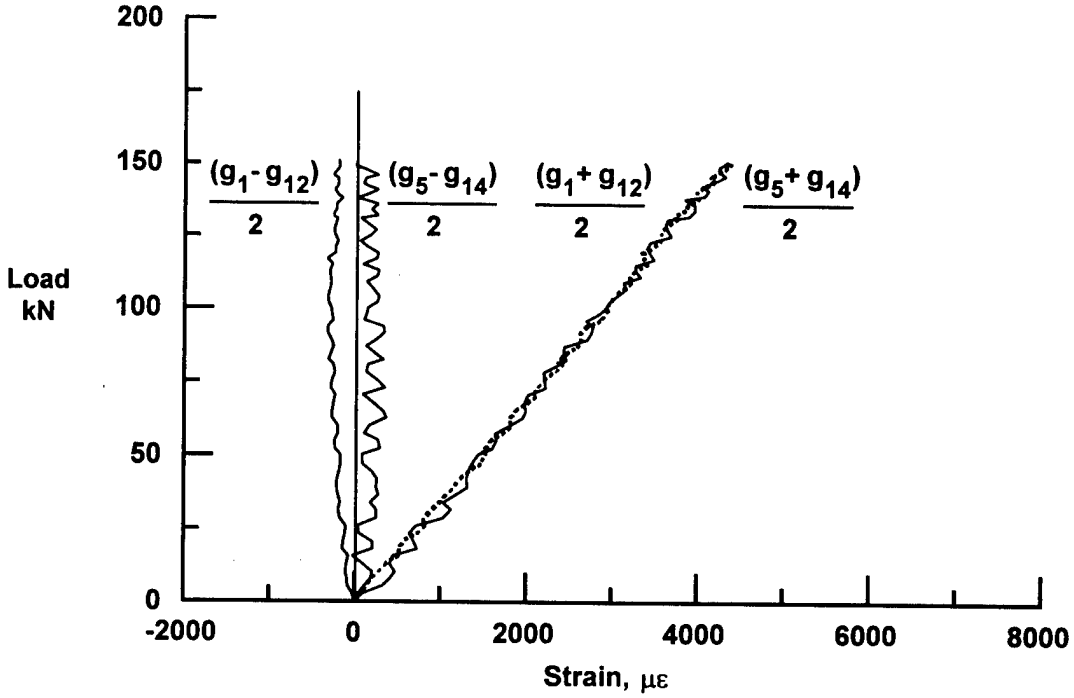

FIGURE A-15. MEMBRANE AND BENDING STRAINS OF WOVEN COMPOSITE PANEL WT0

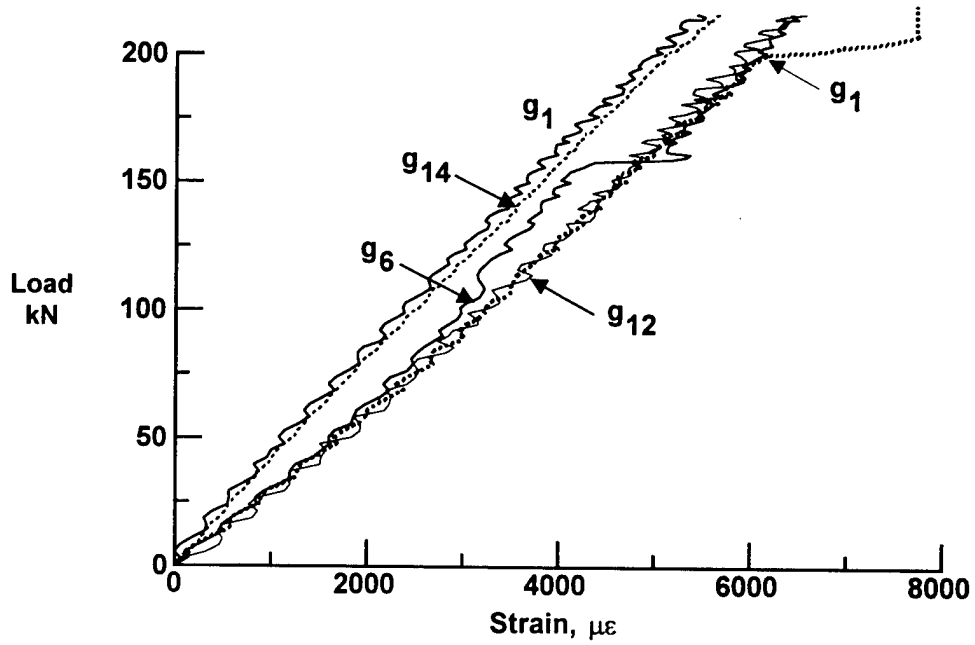

FIGURE A-16. LOAD-STRAIN RESPONSE OF WOVEN COMPOSITE PANEL WT1

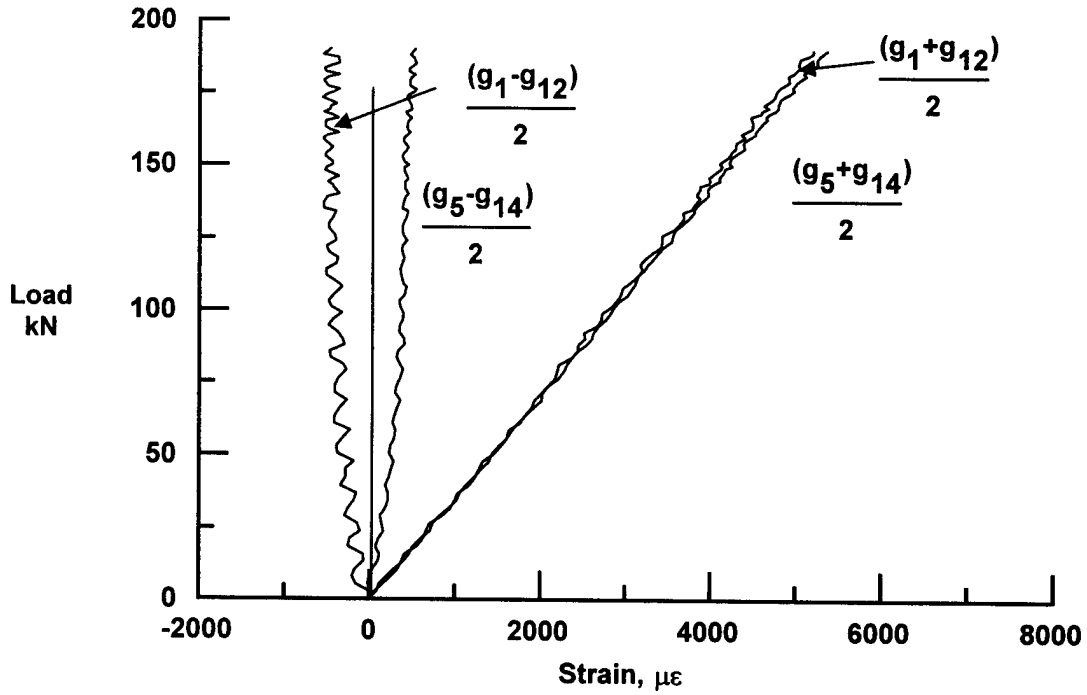

FIGURE A-17. MEMBRANE AND BENDING STRAINS OF WOVEN COMPOSITE PANEL WT1